



## Chronic stress-induced depression-like behaviors through Th1-lymphocytes and microglia-mediated neuroinflammation in the mouse

Cai Zhang<sup>a,b,c</sup>, Baiping Liu<sup>a</sup>, Xiaohong Li<sup>a</sup>, Thierry D. Charlier<sup>c,f</sup>, Kirthana Kunikullaya U<sup>b,c,e</sup>, HarryW.M. Steinbusch<sup>b,\*</sup>, Cai Song<sup>a,d,\*\*</sup>

<sup>a</sup> Research Institute for Marine Drug & Nutrition, College of Food Science & Technology, Guangdong Ocean University, Zhanjiang, China

<sup>b</sup> Department of Cellular and Translational Neuroscience, School for Mental Health and Neuroscience (MHeNs), Faculty of Health, Medicine and Life Sciences, Maastricht University, Maastricht, the Netherlands

<sup>c</sup> Univ Rennes, Inserm, EHESP, Irset (Institut de Recherche en Santé, Environnement et Travail), UMR\_S 1085, F-35000, Rennes, France

<sup>d</sup> Dongguan Mental Health Center/No.7 People's Hospital, Dongguan, China

<sup>e</sup> Department of Physiology, Sri Chamundeshwari Medical College, Hospital and Research Institute, Channarayana, Karnataka, 562160, India

<sup>f</sup> UMR 6552 EthoS CNRS-Univ Rennes-Uni Caen, F-35000, Rennes, France

### ARTICLE INFO

#### Keywords:

Th1 lymphocytes  
Microglia  
p38 MAPK  
Neuroplasticity  
Chronic stress

### ABSTRACT

Recent studies showed the activation of T helper (Th) 1 and microglia during depression. However, the changes in peripheral and central lymphocyte subtypes, and their relationship with microglia in the depression are still unclear. To answer these questions, this study investigated concurrent alterations in lymphocyte subsets (Th1/Th2), microglial activation, and related neuroinflammation and neuronal changes in a mouse model of depression induced by chronic unpredictable mild stress (CUMS). Furthermore, pharmacological inhibitors targeting Th1 (STA-5326), M1 microglia (minocycline), or p38 MAPK (SB203580) were utilized to assess the contribution of these factors to behavioral and molecular outcomes.

CUMS induced significant anhedonia and anxiety-like behaviors. These symptoms were accompanied by a decrease in central CD4 T cells and peripheral CD4/CD8 ratio, alongside an increased Th1/Th2 ratio. Hippocampal levels of cortisol, interleukin (IL)-2, IL-12, and the IFN- $\gamma$ /IL-4 ratio were elevated. CUMS also activated microglia, P38-MAPK pathway and increased neuronal apoptotic signaling (reduced Bcl-2/Bax ratio), and decreased both 5-HT/5-HIAA ratio and neuroplasticity (PSD-95, DCX) in the hippocampus and prefrontal cortex. Notably, the correlations between microglia (Iba-1) and Th1 cell (IL-12), as well as both of them correlations with p-p38 were found. All these parameters were normalized by the three treatments. Interestingly, STA-5326 showed greater efficacy in restoring anhedonia and meningeal CD4 T cell levels, while SB203580 was most effective in normalizing 5-HT neurotransmitter.

In summary, inhibiting Th1 lymphocyte activity, M1-microglia or p-38-MAPK pathways improved depression-like behaviors, which were associated with the normalization of peripheral and central immune imbalances, attenuation of neuroinflammation, and protection of neuroplasticity.

### 1. Introduction

Growing evidence shows that activated peripheral macrophages and some lymphocyte subtypes may induce inflammatory responses and as a consequence participate in the onset and development of depression (Maes et al., 1995; A. Miller, 2010). The discovery of a lymphatic system in the brain (Louveau et al., 2015) further supports the macrophage/lymphocyte hypothesis of depression and underscores the role of

neuroinflammation in the condition.

Activated macrophage or some lymphocyte subtype increase pro-inflammatory cytokine secretion, including T helper (Th) 1 release of pro-inflammatory cytokine interferon- $\gamma$  (IFN- $\gamma$ ), while reducing Th2 anti-inflammatory cytokine interleukin (IL)-4 (Leonard, 2001; Reiche et al., 2005; Zhang et al., 2019a,b; Zhao et al., 2015). Preclinical and clinical studies have demonstrated that depressive symptoms are related to the imbalance between peripheral CD4/CD8 lymphocytes and

\* Corresponding author.

\*\* Corresponding author. Research Institute for Marine Drug & Nutrition, College of Food Science & Technology, Guangdong Ocean University, Zhanjiang, China.  
E-mail addresses: [h.steinbusch@maastrichtuniversity.nl](mailto:h.steinbusch@maastrichtuniversity.nl) (HarryW.M. Steinbusch), [cai.song@dal.ca](mailto:cai.song@dal.ca) (C. Song).

<https://doi.org/10.1016/j.ejphar.2026.178710>

Received 11 September 2025; Received in revised form 31 January 2026; Accepted 27 February 2026

Available online 3 March 2026

0014-2999/© 2026 Elsevier B.V. All rights reserved, including those for text and data mining, AI training, and similar technologies.

Th1/Th2 cytokines. These alterations could be reversed by antidepressant treatments in major depressive disorder (Fan et al., 2019; M Kubera et al., 1999; Myint et al., 2005; Palumbo et al., 2010). More importantly, macrophages and lymphocytes, as well as their produced cytokines are able to cross the BBB to access the central nervous system (CNS) during stress, peripheral inflammation, ageing and malnutrition (Alves de Lima et al., 2020; Engelhardt et al., 2017; Pasciuto et al., 2020b). Proinflammatory cytokines can activate microglia M1 phenotype to release pro-inflammatory cytokines, such as IL-1 $\beta$ , IL-6 and INF- $\gamma$ , and then trigger neuroinflammatory signaling pathways, such as p-38 mitogen-activated protein kinase (MAPK), and finally form inflammatory cascade (Morganti et al., 2019; Pasciuto et al., 2020b; Plastira et al., 2020; Zhu et al., 2010). Proinflammatory cytokines can also stimulate the hypothalamic-pituitary-adrenal (HPA) axis to overproduce corticotropin-releasing factor (CRF) and corticosteroids, which as a consequence activate neuroinflammation (Leonard, 2001; Maes et al., 1995). Furthermore, activated microglia triggered neuroinflammatory responses lead to monoamine neurotransmitter deficiency, including decreased norepinephrine (NE), serotonin (5-HT) and dopamine (DA), as well as the synaptic degeneration including down-regulation of postsynaptic density 95 (PSD-95). These changes are linked to reduced doublecortin (DCX) expression and up-regulated pro-apoptotic Bax expression, all of these changes occurs in depression and associated with depression-like behaviors (Liu et al., 2020; Peng et al., 2020; Sánchez-Vidaña et al., 2019). Although alterations in cytokine profiles associated with various lymphocyte subtypes and the presence of lymphatic vessels have been identified in the brain, the specific abnormalities in peripheral and central lymphocyte populations, as well as their interactions with microglia in depression, particularly in relation to impaired neuroplasticity, remain poorly understood.

To explore the pathway of peripheral immune cells-microglial activation-neuroinflammation-neuroplasticity-depressive-like behaviors, chronic unpredictable mild stress (CUMS)-induced depression model was used (Willner, 2017). The present study to (1) characterize abnormalities in pro- and anti-inflammatory lymphocyte subsets (Th1/Th2), microglial activation, and related neuroinflammatory responses; (2) evaluate the antidepressant effects of STA-5326, minocycline (Mino) and SB203580 on Th1 lymphocytes, M1 microglia and the p38-MAPK pathway, respectively, and then analyzed the potential relationship between hippocampal Iba-1 or IL-12 and p-p38; and (3) compare the effects of these three interventions to inform potential therapeutic strategies for major depressive disorder.

## 2. Materials and methods

### 2.1. Animals

Sixty-five C57 male mice (5 weeks old, Changsha Tianqin Biotechnology Co., Ltd, China) were housed in groups of three to five per cage with a 12 h light/dark cycle (lights on at 7:00 and off at 19:00), room temperature  $23 \pm 1$  °C and humidity  $50 \pm 10\%$  at Guangdong Ocean University animal facility (SYXK (Yue) 2014-0053). Animals were fed standard rodent chows with water available *ad libitum*. Prior to the experiment, mice were acclimated to the laboratory for seven days. The experiment protocol was approved by the Institutional Bioethics Committee (Guangdong Ocean University, China, IACUC-20190513-012) according to National Institutes of Health Guide for the Care and Use of the Laboratory Animals.

### 2.2. Experimental procedure

The male mice were divided into 8 experimental groups as CT (Control, n = 10), Mino (Minocycline, n = 5), SB203580 (n = 5), STA-5326 (n = 5), CUMS (Stress, n = 10), CUMS + Mino (n = 10), CUMS + SB203580 (n = 10) and CUMS + STA-5326 (n = 10). Mino, SB203580 and STA-5326 are microglia, MAPK (P38) and Th1 inhibitors,

respectively. Fig. 1 represents the study design. Mice were subjected to CUMS for 81 days. Vehicle consists of final concentration 5% DMSO and 10% Sulfolbutylether beta-cyclodextrin (SBE- $\beta$ -CD) dissolved in saline. During days 57-80 of the study, Mino (40 mg/kg, dissolved in saline, Shanghai Yuanye Biotechnology Co., Ltd, 13614-98-7, China), STA-5326 (7 mg/kg, dissolved in vehicle, Shanghai Binghui Chemical Technology Co., Ltd, 541550-19-0, China) and SB203580 (5 mg/kg, dissolved in vehicle, ApexBio, A8254, USA) were i.p. injected daily. CT, CUMS, Mino and CUMS + Mino groups were i.p. injected with equal amounts of vehicle. During days 73-76, the sucrose preference test (SPT) was performed. During days 78-79, the elevated plus maze test (EPT) was conducted between 7:30-13:30. Mice were euthanized by Zoletil after one day of rest (Fig. 1).

### 2.3. Stress exposure paradigms

The CUMS protocol was described previously with mild modification in this study (Zhang et al., 2019a,b). Thirteen different stressors were applied (2 stressors per day) in a random order over a period of 81 days, including cold 4 °C for 1.5 h, swimming at 17 °C for 10 min, rotation 3 h, isolation overnight, restraint for 1.5 h, cage tilt 45 °C overnight, stroboscopic light overnight, light overnight exposure, crowding 4 h, odor 12 h, empty bottle stimulates 24 h, food deprivation 24 h, and wet bedding for 12 h.

### 2.4. Sucrose preference test

Anhedonia behavior was measured by sucrose preference test as previously described (Gu et al., 2018). On day 1, mice were offered two bottles of 1% (w/v) sucrose water to consume at 19:00 for 24 h. On day 2, mice were offered one bottle of 1% sucrose water and one bottle of fresh water at 19:00 for 24 h. On day 3, food and water deprivation at 19:00 for 24 h and on day 4 mice were offered one bottle 1% sucrose water and one bottle fresh water at 19:00, then the consumption of sucrose water and fresh water after 4 h was weighed. Sucrose preference (SP) was calculated according to the following formula,  $SP = \frac{\text{sucrose intake}}{\text{sucrose intake} + \text{water intake}} \times 100\%$ .

### 2.5. Elevated plus maze

Anxiety-related behavior was measured by EPM test as described previously (Zhang et al., 2019a,b). In brief, mice were placed on the central platform facing the same open arm and anxiety-related behaviors were recorded by the SuperMaze behavior analysis system (Shanghai Xinruan Information Technology Co., Ltd, Shanghai, China) for 5 min by two highly trained observers blinded to the groups. Before the test, mice were acclimated to the room for 0.5 h, and the arena was cleaned with 0.5% EtOH after every trial. The number of entries into the open (open N) and closed (close N) arms and the time spent on open (open T) and closed (close T) arms, as well as the ratios of number and time of close/open were quantified.

### 2.6. Collection of samples and assay

One day after behavioral testing, the animals were anesthetized and euthanasia. All spleen, thymus and meninges samples were collected for flow cytometry, while three whole brains from each group (Mino, SB203580 and STA-5326 groups not collected) were collected with 4% paraformaldehyde (Solarbio, Beijing, China) for immunohistochemistry. The remaining seven brains were rapidly dissected into the hippocampus and the frontal cortex, and snapped freeze with liquid nitrogen and subsequently store them at  $-80$  °C until homogenization for HPLC, ELISA and Western blot assays.

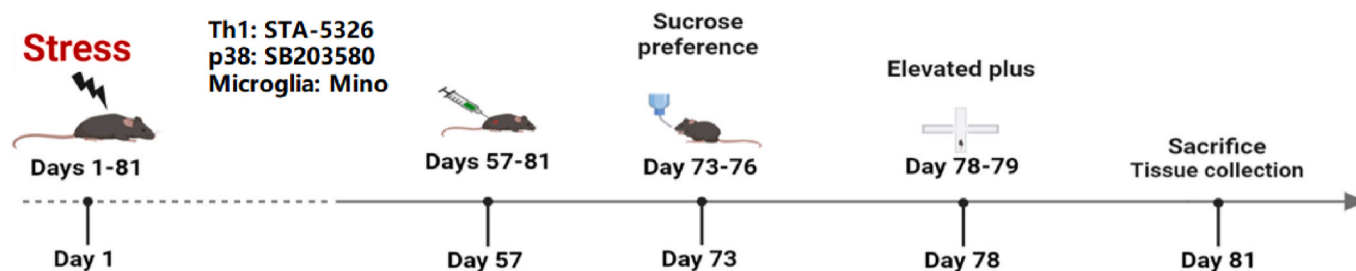


Fig. 1. Experiment process.

## 2.7. ELISA assay

Hippocampal tissues were weighed and homogenized in ice-cold  $1 \times$  PBS at a ratio of 10% (w/v) (1 g tissue + 9 mL PBS). The homogenates were centrifuged at 4500 r/min for 15 min at  $4^\circ\text{C}$ , and the supernatants were collected for subsequent analysis. Total protein concentration was determined by a BCA protein assay kit (Beijing dingguo changsheng Co., Ltd, China) according to the manufacturer's instructions. This value was used to normalize the target protein levels to total protein content in subsequent ELISA measurements. The commercially available mouse ELISA kits (Jiangsu Yutong Biotechnology Co., Ltd, China) were used to determine cytokines IL-2 (MM-0701M1), IL-4 (MM-0165M1), IL-12 (MM-0105M1), IFN- $\gamma$  (MM-0182M1), Iba-1 (MM-44902M1), p-p38 (MM-44666M1), CORT (MM-0061M1), Bcl-2 (MM-0306M1) and Bax (MM-44811M1) in hippocampal supernatant samples according to the manufacturer's protocols.

## 2.8. The analysis of spleen and thymus T-lymphocyte subtypes by flow cytometer

The spleen and thymus were harvested after the mice were euthanized. Lymphocytes were immediately extracted from the spleen and thymus by Lymphocyte Separation Medium (Tianjin Haoyang biological products Technology Co., Ltd, China). The single lymphocyte suspension ( $2 \times 10^6/100 \mu\text{L}$ ) was stained with CD4<sup>+</sup> PC5 (15-0041-81, eBioscience), IFN- $\gamma$ -APC (17-7311-81, eBioscience) and IL-4-PE (12-7041-81, eBioscience) for 30 min at  $4^\circ\text{C}$  in dark. After washing according to the manufacturer protocols, the samples were detected and analyzed by CytoFLEX (Beckman, China).

## 2.9. The analysis of meninges T-lymphocyte isolates by flow cytometer

Mice were transcardially perfused with 1X PBS for 15 min. Animal heads were removed and skulls were quickly stripped of all flesh. Mandibles were then removed, as well all skull material rostral to maxillae. Surgical scissors were used to remove skull tops, cutting clockwise, beginning, and ending inferior to the right post tympanic hook. Brains and skulls were immediately placed into ice-cold RPMI-1640 (Thermo Fisher Scientific, China). Meninges (dura, arachnoid, and pia mater) were carefully removed from the interior aspect of skulls and surfaces of brains with forceps. Meninges were enzymatically dissociated with 2 mg/ml collagenase D (Roche Applied Science) and 2 mg/ml DNase I (Roche Applied Science) in PBS for 45 min at  $37^\circ\text{C}$ . Then meningeal tissue was gently pressed through  $70 \mu\text{m}$  nylon mesh cell strainers with sterile plastic plungers to yield a single cell suspension. Cells were centrifuged at 500 g at  $4^\circ\text{C}$  for 10 min, the supernatant was removed, and cells were resuspended in ice-cold flow cytometry Staining buffer. Isolated cells were stained with CD4-PC5 (15-0041-81, eBioscience) for 30 min at  $4^\circ\text{C}$  in the dark. After washing with flow cytometry staining buffer, the samples (2-3 meninges from each group were pooled) were detected and analyzed by CytoFLEX (Beckman, China).

## 2.10. Immunofluorescence

Mice were transcardially perfused with cold 1x PBS for 15 min. Three brains per group were immersion fixed by 4% PFA at  $4^\circ\text{C}$  for 24 - 48 h, and then cryoprotected with 30% sucrose until the brain sank to the bottom of the tube, then dried and stored at  $-80^\circ\text{C}$  until using. The brains were cut into slices of  $15 \mu\text{m}$  through hippocampal area with a cryostat (Kedi, Jinhua, China). The slices were fixed in 4% PFA for 0.5 h at room temperature. After rinsing in PBST, these slices were incubated in primary antibody Iba-1, rabbit (Wako, 01919741, 1:400) at  $4^\circ\text{C}$  for overnight. Slices were rinsed in PBST, and then incubated in secondary antibody with Alexa Fluor 488-conjugated goat anti-rabbit IgG (Abcam, ab150081, 1:300) at RT for 2 h. DAPI (Biomol,  $1 \mu\text{g}/\text{mL}$ ) was used for nuclear counter staining. The fluorescent images of Iba-1 were captured by a fluorescence microscope system (Leica DM2500, Germany). The images were analyzed with ImageJ (NIH) software.

## 2.11. Western blots

According to the manufacturer's instructions, the total protein of hippocampus and PFC was extracted with a commercial kit (Beijing dingguo changsheng Co., Ltd, China). The concentration of the protein was measured with BCA kit (Beijing dingguo changsheng Co., Ltd, China). Subsequently, 30-50  $\mu\text{g}$  protein was loaded onto a 10% polyacrylamide gel, and then transferred to PVDF (Millipore, China) membrane. After incubation with Western blot blocking solution reagent (Millipore, China) at room temperature for 2 h, membranes were incubated with primary antibody overnight at  $4^\circ\text{C}$ . After washing, the membranes were further incubated with secondary antibodies for 2 h, washing and detection using enhanced chemiluminescence (Millipore, China). The bands were scanned and analyzed using a chemiluminescence system (Tanon 5200, Shanghai, China). The mouse origin antibodies for P-erk (sc-7383, 42-44 kDa, 1:400), DCX (sc-271390, 40 kDa, 1:400), PSD95 (sc-32290, 95 kDa, 1:400) and  $\beta$ -Actin (sc-47778, 43 kDa, 1:400) were purchased from Santa Cruz Biotechnology (Santa Cruz, CA, USA). All target proteins were quantified by normalizing them to  $\beta$ -actin re-probed on the same membrane and then calculated as a percentage of the control group.

## 2.12. HPLC analysis of monoamine neurotransmitters and metabolites

Hippocampal tissue was homogenized in 0.60 M ice-cold perchloric acid containing 50 mM  $\text{Na}_2\text{EDTA}$  with 100 ng isoproterenol as an internal standard. The homogenates were centrifuged twice at 14,000 rpm/min for 15 min at  $4^\circ\text{C}$ . Supernatants were filtered with  $0.45 \mu\text{m}$  membrane and transferred to new tubes. The PH of supernatants was adjusted to 3.8 with 1 M sodium acetate, and then supernatants were stored at  $-80^\circ\text{C}$  until use. For the HPLC analysis,  $10 \mu\text{L}$  of the pH-adjusted supernatant was injected into an HPLC system with fluorescence detection (Agilent, Santa Clara, CA, USA). The neurotransmitters and their metabolites in samples were separated by a C18 reverse-phase column ( $4.5 \times 150 \text{ mm}$ ) (Agilent, Santa Clara, CA, USA) with a mobile phase containing sodium acetate and citric acid. The mobile phase was

prepared as follow: 0.1 M sodium acetate was mixed 0.1 M citric acid in a 10:9 ratio, and adjusted to PH 3.5 (0.1 M sodium citric buffer), mixed with methanol in a ratio of 85:15 and then supplemented with sodium octane sulfonate (100 mg/L), Na<sub>2</sub>EDTA (5 mg/mL), Dopamine (DA), NE, 3-methoxy-4-hydrophenyl (MHPG), 5-HT, and 5-hydroxyindole-3-acetic acid (5-HIAA) were analyzed (Peng and Zhang, 2020).

### 2.13. Statistical analysis

All data were expressed as mean  $\pm$  SEM and analyzed by SPSS 20.0 software. Parametric data were measured by two-way analysis of variance (ANOVA) with factors CUMS (stress/control) and treatment (drug/saline) followed by Fisher LSD *post-hoc* test. Non-parametric data were analyzed by Kruskal-Wallis test, and followed by a Bonferroni-corrected *post-hoc* Wilcoxon- Mann-Whitney *U* test. The correlations between several pairs of parameters were analyzed by Pearson correlation analysis. Significance was set at  $P < 0.05$  in all tests.

## 3. Results

### 3.1. CUMS-induced anhedonia was reversed by Mino, SB203580 or STA-5326

There was a significant interaction ( $F_{3,57} = 6.476$ ,  $P < 0.01$ ) between CUMS and treatments in the sucrose preference. The *post hoc* test revealed CUMS ( $P < 0.01$ ) induced anhedonia, while Mino ( $P < 0.01$ ), SB203580 ( $P < 0.01$ ) or STA-5326 ( $P < 0.01$ ) treatment improved anhedonia-like behavior (Fig. 2). Moreover, compared to SB203580 ( $P = 0.055$ ) and Mino ( $P < 0.05$ ), STA-5326 treatment was more significant to improve anhedonia behavior.

### 3.2. CUMS-induced anxiety-like behaviours were reversed by Mino, SB203580 or STA-5326

Two-way ANOVA showed CUMS decreased the number of mouse entry into open arms ( $F_{1,57} = 5.207$ ,  $P < 0.05$ ) and the ratio of entries into open/close arms ( $F_{1,57} = 19.801$ ,  $P < 0.01$ ). Mino, SB203580 or STA-5326 treatment increased open arm entries ( $F_{3,57} = 5.122$ ,  $P < 0.01$ ) and ratio of open/closed arm entries ( $F_{3,57} = 5.159$ ,  $P < 0.01$ ) (Fig. 3A–C). The Kruskal-Wallis test showed CUMS significantly decreased the time spent on the open arm ( $H = 16.948$ ,  $P < 0.01$ ) and the ratio of open/close time spent ( $H = 20.884$ ,  $P < 0.01$ ). The *post hoc* test revealed CUMS ( $P < 0.05$ ) can result in anxiety-like behaviors, such

as decreased open T and the ratio T, while Mino ( $P < 0.01$ ), SB203580 ( $P < 0.05$ ) or STA-5326 ( $P < 0.01$ ) treatment reversed these changes (Fig. 3B and C).

### 3.3. CUMS-increased peripheral Th1/Th2 ratio was reversed by Mino, SB203580 or STA-5326

Kruskal-Wallis test showed CUMS significantly decreased the ratio of CD4<sup>+</sup>/CD8<sup>+</sup> (CD4<sup>+</sup>/CD4<sup>-</sup>) ( $H = 10.67$ ,  $P < 0.05$ ) in the thymus, and increased both Th1/Th2 (CD4<sup>+</sup>IFN- $\gamma$ +/CD4<sup>+</sup>IL-4+) ratio in the spleen ( $H = 10.51$ ,  $P < 0.05$ ) and thymus ( $H = 12.21$ ,  $P < 0.05$ ). The *post hoc* test revealed CUMS ( $P < 0.05$ ) induced the abnormalities in peripheral T lymphocytes (including decreased CD4<sup>+</sup>/CD8<sup>+</sup> ratio and increased Th1/Th2 ratio). Mino ( $P < 0.05$ ), STA-5326 ( $P < 0.05$ ) or SB203580 ( $P < 0.05$ ) treatment significantly increased thymic CD4<sup>+</sup>/CD8<sup>+</sup> ratio. Moreover, Mino ( $P < 0.05$ ), SB203580 ( $P < 0.01$ ) or STA-5326 ( $P < 0.05$ ) treatment reversed the Th1/Th2 ratio in the spleen. Interestingly, compared to Mino, SB203580 ( $P < 0.01$ ) or STA-5326 ( $P < 0.05$ ) treatments significantly decreased thymic Th1/Th2 ratio (Table 1).

### 3.4. CUMS decreased meningeal CD4 lymphocytes and increased hippocampal IL-2 and IL-12 concentration, which were reversed by Mino, SB203580 or STA-5326

In the hippocampus, a significant interaction between CUMS and treatments appeared in the concentration of lymphocyte growth factor IL-2 ( $F_{3,42} = 8.291$ ,  $P < 0.01$ ) and Th1 lymphocyte stimulating factor IL-12 ( $F_{3,42} = 4.927$ ,  $P < 0.01$ ). The *post hoc* test revealed that CUMS significantly increased IL-2 ( $P < 0.01$ ) and IL-12 ( $P < 0.01$ ) concentrations. However, Mino ( $P < 0.01$ ), STA-5326 ( $P < 0.01$ ), or SB 203580 ( $P < 0.01$ ) treatment equally reversed these changes (Fig. 4C and D). Furthermore, CUMS significantly reduced CD4 lymphocyte number ( $H = 23.081$ ,  $P < 0.01$ ) in the meninges, which were increased by Mino ( $P < 0.01$ ), SB203580 ( $P < 0.01$ ) or STA-5326 ( $P < 0.01$ ) treatment (Fig. 4B). Moreover, the effect of STA-5326 was stronger than SB203580 ( $P < 0.05$ ) and Mino ( $P = 0.06$ ) on the meninges CD4 cell decrease.

### 3.5. CUMS increased central corticosteroid concentration, which were reversed by Mino, SB203580 or STA-5326

There was a significant interaction between CUMS and treatments in hippocampal corticosterone (CORT) concentrations ( $F_{3,42} = 3.267$ ,  $P < 0.05$ ) (Fig. 5). The *post hoc* test revealed CUMS ( $P < 0.01$ ) increased

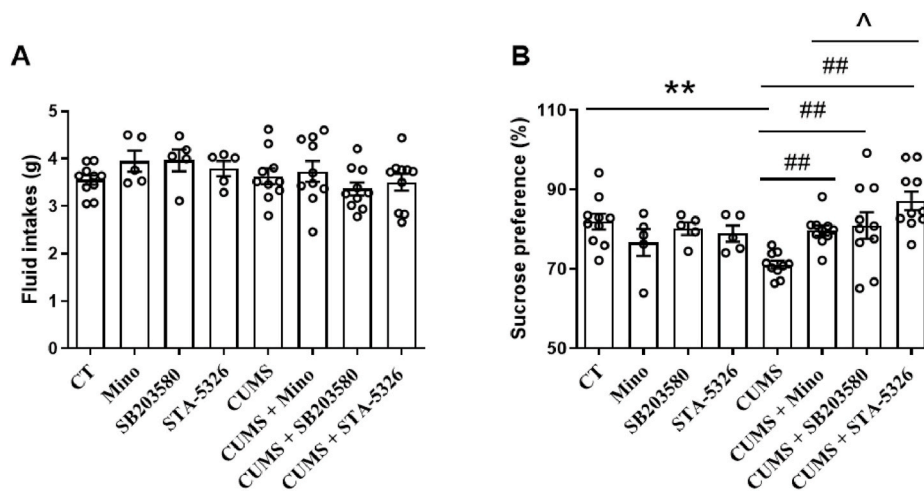
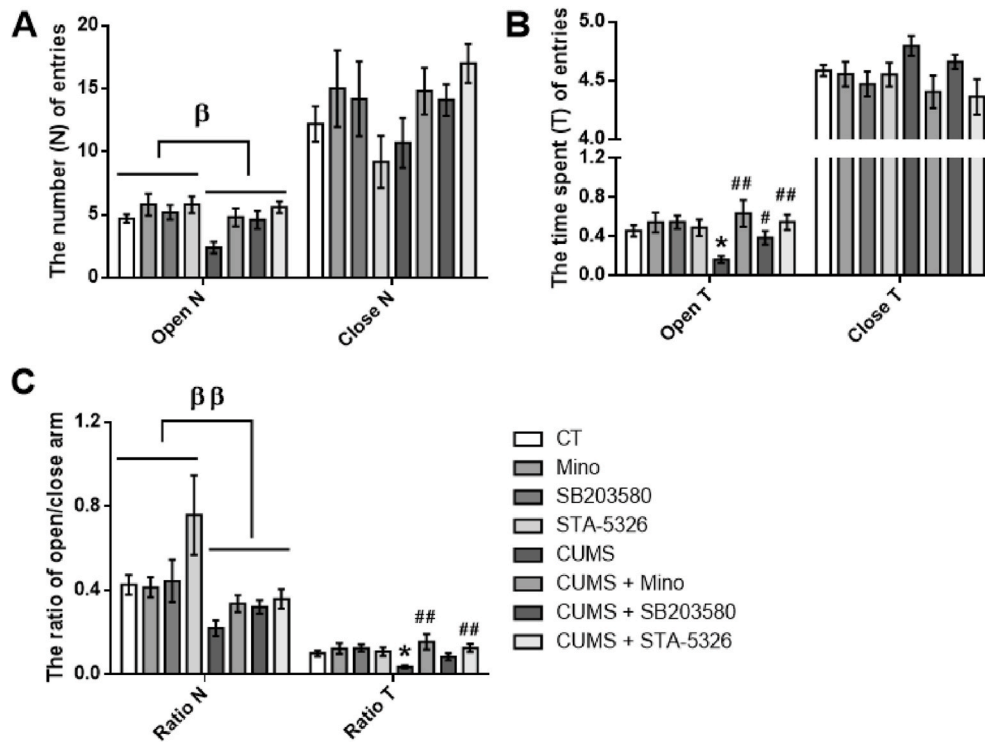


Fig. 2. Mino, SB203580 or STA-5326 reversed CUMS-induced anhedonia. A) The total consumption of water and sucrose water by mice. B) The sucrose preference (%). Data are expressed as the mean  $\pm$  SEM.  $N = 5$  for Mino, SB203580 and STA-5326 groups,  $N = 10$  for remaining groups. \*\* $P < 0.01$  vs. control; ## $P < 0.01$  vs. CUMS; ^ $P < 0.05$  CUMS + STA-5326 vs. CUMS + Mino.



**Fig. 3.** Mino, SB203580 or STA-5326 improved CUMS induced anxiety in the elevated plus maze test. A) The number of mouse enter into the open (Open N) and close arm (Close N). B) The time spent on the open (Open T) and close arm (Close T). C) The number (Ratio N) and time ratio (Ratio T) of open/close. All data are expressed as the mean  $\pm$  SEM. N = 5 for Mino, SB203580 and STA-5326 groups, N = 10 for remaining groups.  $^{\beta}P < 0.05$ ,  $^{\beta\beta}P < 0.01$  CUMS main effect.  $^*P < 0.05$  vs. control;  $^{##}P < 0.01$  vs. CUMS.

**Table 1**  
Lymphocyte subtype changes in the spleen and thymus.

Lymphocytes		CD3 <sup>+</sup> CD4 <sup>+</sup>	CD3 <sup>+</sup> CD4 <sup>-</sup>	CD4/CD4-	CD4+IFN- $\gamma$ +	CD4+IL-4+	IFN- $\gamma$ /IL-4
Spleen	CT	55.45 $\pm$ 0.48	44.55 $\pm$ 0.48	1.25 $\pm$ 0.02	11.2 $\pm$ 1.07	0.84 $\pm$ 0.15	15.2 $\pm$ 2.88
	Mino	54.98 $\pm$ 2.11	45.02 $\pm$ 2.11	1.23 $\pm$ 0.1	14.87 $\pm$ 2.82	0.78 $\pm$ 0.17	21.84 $\pm$ 8.41
	SB203580	55.72 $\pm$ 0.7	44.28 $\pm$ 0.7	1.26 $\pm$ 0.04	9.84 $\pm$ 1.33	0.68 $\pm$ 0.09	14.87 $\pm$ 2.34
	STA-5326	54.5 $\pm$ 2.05	45.5 $\pm$ 2.05	1.21 $\pm$ 0.1	9.94 $\pm$ 0.74	0.82 $\pm$ 0.25	14.03 $\pm$ 3.19
	CUMS	52.62 $\pm$ 0.94	47.38 $\pm$ 0.94	1.11 $\pm$ 0.04	11.1 $\pm$ 0.34	0.42 $\pm$ 0.02	26.71 $\pm$ 1.62 <sup>**</sup>
	CUMS + Mino	54.42 $\pm$ 1.38	45.58 $\pm$ 1.38	1.2 $\pm$ 0.07	12.7 $\pm$ 1.04	0.75 $\pm$ 0.07	17.76 $\pm$ 2.37 <sup>#</sup>
	CUMS + SB203580	56.86 $\pm$ 0.87	43.14 $\pm$ 0.87	1.32 $\pm$ 0.04	10.51 $\pm$ 0.91	0.88 $\pm$ 0.14	12.59 $\pm$ 1.21 <sup>##</sup>
	CUMS + STA-5326	53.94 $\pm$ 1.11	46.06 $\pm$ 1.11	1.18 $\pm$ 0.05	10.79 $\pm$ 1.65	0.66 $\pm$ 0.13	18.06 $\pm$ 2.64 <sup>#</sup>
Thymus	CT	82.6 $\pm$ 0.74	17.4 $\pm$ 0.74	4.78 $\pm$ 0.22	0.92 $\pm$ 0.16	0.83 $\pm$ 0.15	1.27 $\pm$ 0.29
	Mino	81.63 $\pm$ 0.67	18.37 $\pm$ 0.67	4.46 $\pm$ 0.2	1 $\pm$ 0.19	1.83 $\pm$ 1.13	1.45 $\pm$ 0.83
	SB203580	81.7 $\pm$ 1.47	18.3 $\pm$ 1.47	4.53 $\pm$ 0.45	1.05 $\pm$ 0.51	0.68 $\pm$ 0.22	1.42 $\pm$ 0.28
	STA-5326	84.02 $\pm$ 2.13	15.98 $\pm$ 2.13	5.52 $\pm$ 0.98	1.11 $\pm$ 0.14	1.23 $\pm$ 0.06	0.9 $\pm$ 0.09
	CUMS	79.72 $\pm$ 0.57	20.28 $\pm$ 0.57	3.95 $\pm$ 0.14 <sup>*</sup>	1.56 $\pm$ 0.49	0.56 $\pm$ 0.14	2.65 $\pm$ 0.41 <sup>*</sup>
	CUMS + Mino	81.75 $\pm$ 0.48	18.25 $\pm$ 0.48	4.5 $\pm$ 0.16 <sup>#</sup>	1.26 $\pm$ 0.18	0.57 $\pm$ 0.16	2.58 $\pm$ 0.5
	CUMS + SB203580	82.04 $\pm$ 0.61	17.96 $\pm$ 0.61	4.59 $\pm$ 0.18 <sup>#</sup>	0.97 $\pm$ 0.08	1.24 $\pm$ 0.27	0.93 $\pm$ 0.19 <sup>##, <math>\gamma\gamma</math></sup>
	CUMS + STA-5326	82.57 $\pm$ 0.65	17.43 $\pm$ 0.65	4.77 $\pm$ 0.21 <sup>#</sup>	0.79 $\pm$ 0.1	0.67 $\pm$ 0.09	1.3 $\pm$ 0.25 <sup>#, <math>\wedge</math></sup>

All data are expressed as the mean  $\pm$  SEM (N = 5 per group, 2 spleen or thymus from each group were pooled).  $^*P < 0.05$ ,  $^{**}P < 0.01$  vs. control;  $^{\#}P < 0.05$ ,  $^{##}P < 0.01$  vs. CUMS;  $^{\gamma\gamma}P < 0.01$  CUMS + SB203580 vs. CUMS + Mino;  $^{\wedge}P < 0.05$  CUMS + STA-5326 vs. CUMS + Mino.

hippocampal CORT concentrations, while Mino ( $P < 0.01$ ), SB203580 ( $P < 0.01$ ) or STA-5326 ( $P < 0.01$ ) treatment significantly reversed CUMS effects.

**3.6. CUMS-activated central MAPK pathway was reversed by Mino, SB203580 or STA-5326**

There was a significant interaction between CUMS and treatments in hippocampal P-p38 Concentration ( $F_{3,42} = 3.058$ ,  $P < 0.05$ ). A significant main effect of treatments were also found both in PFC ( $F_{3,31} = 3.73$ ,  $P < 0.05$ ) and hippocampal P-erk protein ( $F_{3,31} = 5.86$ ,  $P < 0.01$ )

(Fig. 6B and C). The *post hoc* test indicated that CUMS significantly increased the concentration of P-p38 ( $P < 0.01$ ), and the change was attenuated by Mino ( $P < 0.01$ ), SB203580 ( $P < 0.01$ ) or STA-5326 ( $P < 0.01$ ) treatment (Fig. 6A).

**3.7. CUMS-increased hippocampal Iba-1 concentration and Th1/Th2 ratio were reversed by Mino, SB203580 or STA-5326**

A significant interaction between CUMS and treatments in the concentration of microglia marker Iba-1 ( $F_{3,42} = 3.223$ ,  $P < 0.05$ ) and IFN- $\gamma$ /IL-4 (Th1/Th2) ratio ( $F_{3,42} = 5.141$ ,  $P < 0.01$ ) were found in the

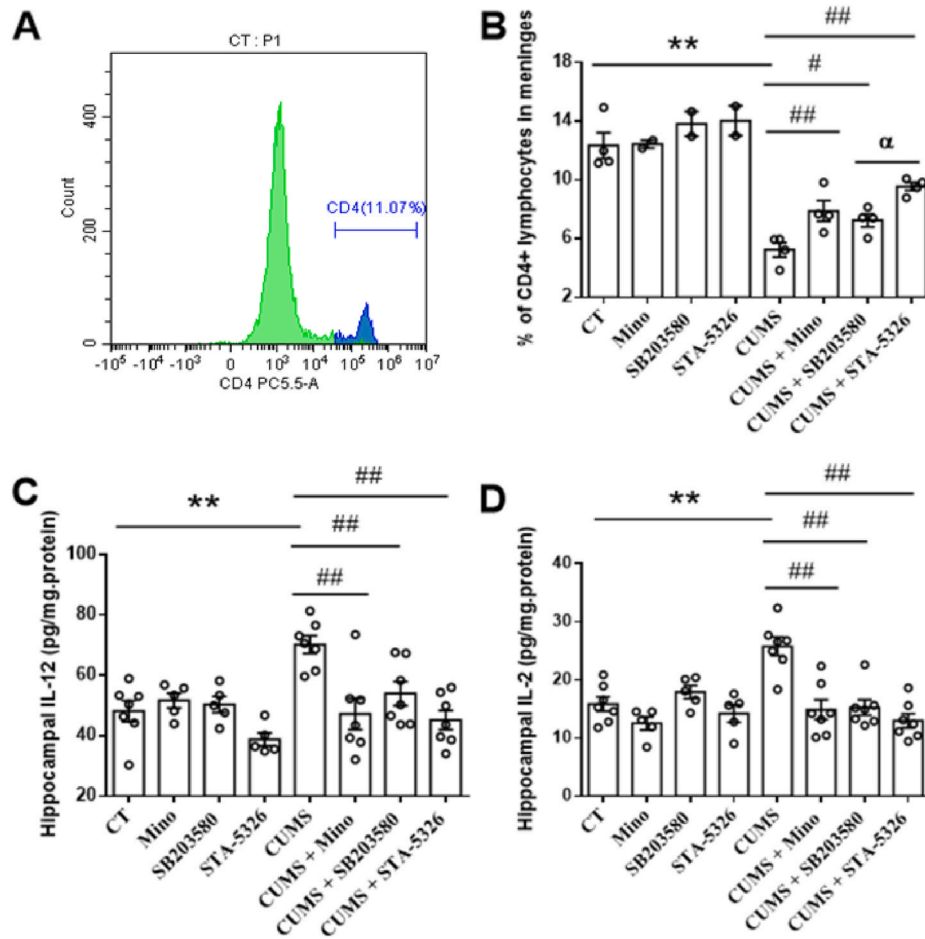


**Fig. 4.** Mino, SB203580 or STA-5326 improved CUMS-induced abnormal changes in meningeal CD4 lymphocytes and hippocampal IL-2 and IL-12 concentrations. A) Histogram of meninges CD4 by Flow cytometry. B) The percent of CD4 in meninges. C) Hippocampal IL-12 concentration. D) Hippocampal IL-2 concentration. All data are expressed as the mean  $\pm$  SEM. B: meningeal samples 5 animals in each group were pooled as N = 2 for Mino, SB203580 and STA-5326 groups, N = 4 for remaining groups; C and D: N = 5 for Mino, SB203580 and STA-5326 groups, N = 7 for remaining groups. \*\* $P < 0.01$  CUMS vs. control; # $P < 0.05$ , ## $P < 0.01$  vs. CUMS;  $\alpha P < 0.05$  CUMS + STA-5326 vs. CUMS + SB203580.

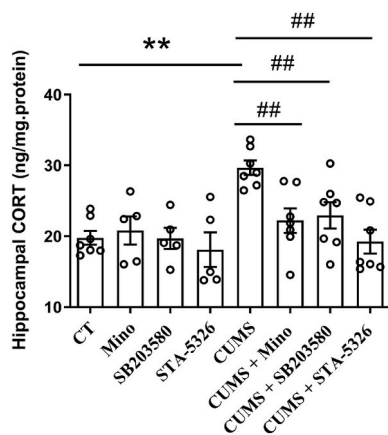


**Fig. 5.** Mino, SB203580 or STA-5326 improved CUMS-induced increase in CORT level in the hippocampus. All data are expressed as the mean  $\pm$  SEM. N = 5 per group for Mino, SB203580 and STA-5326 groups, N = 7 for remaining groups. \*\* $P < 0.01$  CUMS vs. control; ## $P < 0.01$  vs. CUMS.

hippocampus. There was also a significant main effect of CUMS in Th1 cytokine IFN- $\gamma$  ( $F_{1,42} = 21.281$ ,  $P < 0.01$ ) and Th2 cytokine IL-4 ( $F_{1,42} = 11.473$ ,  $P < 0.01$ ) concentration (Fig. 7C and D). Mino, SB203580 or STA-5326 treatment reduced CUMS-induced increase in IFN- $\gamma$  ( $F_{3,42} =$

3.582,  $P < 0.05$ ). The *post hoc* test revealed that CUMS significantly increased the concentration of Iba-1 ( $P < 0.01$ ) and IFN- $\gamma$ /IL-4 ratio ( $P < 0.01$ ). Mino ( $P < 0.01$ ), SB203580 ( $P < 0.01$ ) or STA-5326 ( $P < 0.01$ ) treatment significantly reduced the ratio (Fig. 7B-E).

### 3.8. CUMS-induced abnormalities of neurotransmitters was reversed by Mino, SB203580 or STA-5326

In the hippocampus, there was a significant interaction between CUMS and treatments in 5-HT ( $F_{3,37} = 5.449$ ,  $P < 0.01$ ), DA ( $F_{3,37} = 3.465$ ,  $P < 0.05$ ) NE ( $F_{3,37} = 2.81$ ,  $P < 0.01$ ) and 5-HT/5-HIAA ( $F_{3,37} = 6.913$ ,  $P < 0.01$ ). The *post hoc* test revealed CUMS significantly decreased hippocampal 5-HT ( $P < 0.01$ ), DA ( $P < 0.01$ ), NE ( $P < 0.01$ ) and the ratio of 5-HT/5-HIAA ( $P < 0.01$ ). Mino, SB203580 or STA-5326 treatment partly reversed these alterations. Interestingly, the effect of SB203580 was better than Mino in normalizing 5-HT/5-HIAA ratio ( $P < 0.05$ ), and also more effective than Mino ( $P < 0.01$ ) and STA-5326 ( $P < 0.05$ ) in restoring 5-HT concentration (Table 2).

In the PFC, there was also a significant interaction between CUMS and treatments in 5-HT/5-HIAA ( $F_{3,37} = 3.026$ ,  $P < 0.01$ ). The Kruskal-Wallis test also showed CUMS and treatments significantly affected NE ( $H = 11.1$ ,  $P < 0.05$ ) and 5-HT ( $H = 9.61$ ,  $P < 0.05$ ) concentrations. The *post hoc* test revealed that CUMS significantly decreased NE ( $P < 0.05$ ) and 5-HT ( $P < 0.05$ ) concentrations, as well as the ratio of 5-HT/5-HIAA ( $P < 0.01$ ). Mino, SB203580 or STA-5326 treatment partly alleviated

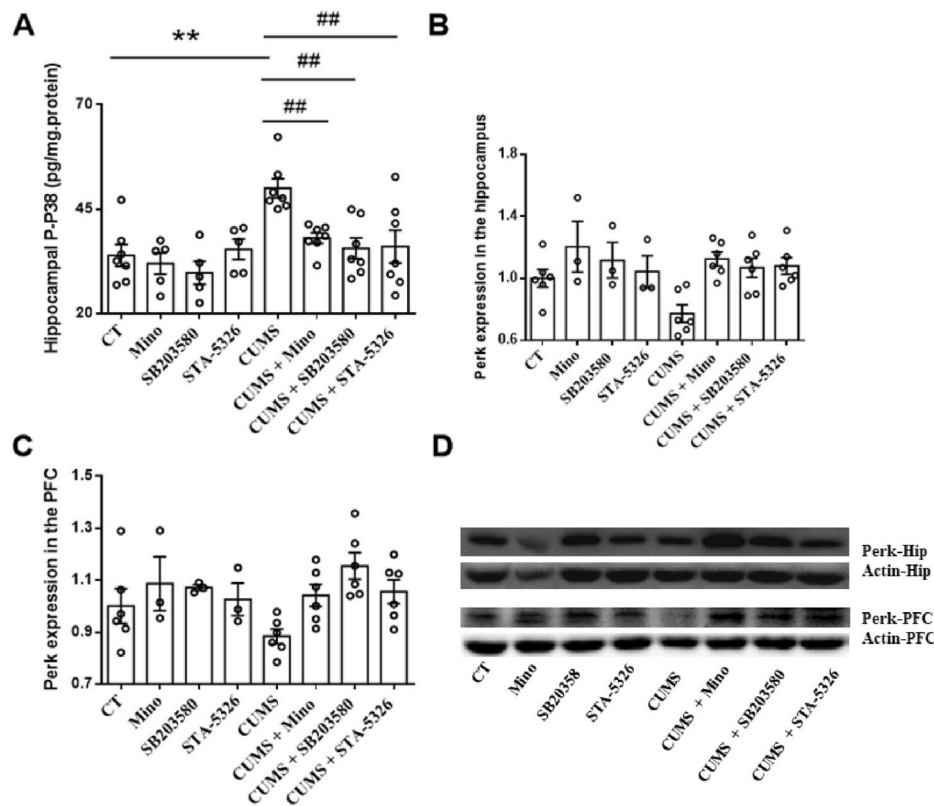


**Fig. 6.** Mino, SB203580 or STA-5326 reversed CUMS-induced MAPK activation in the hippocampus and PFC. A) P-p38 concentration in the hippocampus; B) P-erk expression in the hippocampus; C) P-erk expression in the PFC; D) WB band of Perk expression. All data are expressed as the mean  $\pm$  SEM. A: N = 5 for Mino, SB203580 and STA-5326 groups, N = 7 for remaining groups; B and C: N = 3 for Mino, SB203580 and STA-5326 groups, N = 6 for remaining groups. \*\* $P < 0.01$  CUMS vs. control; ## $P < 0.01$  vs. CUMS.

these changes. While, compared to Mino ( $P < 0.01$ ) and STA-5326 ( $P < 0.05$ ), SB203580 treatment significantly increased 5-HT concentration and 5-HT/5-HIAA ratio in the hippocampus or PFC (Table 2).

### 3.9. CUMS-reduced neuroplasticity was reversed by Mino, SB203580 or STA-5326

There was a significant interaction between CUMS and treatments in DCX (Hip:  $F_{3,31} = 5.12$ ,  $P < 0.01$ ) and PSD-95 (Hip:  $F_{3,31} = 4.42$ ,  $P < 0.05$ , PFC:  $F_{3,31} = 3.47$ ,  $P < 0.05$ ). The *post hoc* test revealed CUMS significantly down-regulated PSD-95 ( $P < 0.01$ ) and DCX ( $P < 0.01$ ) expression in the hippocampus (Fig. 8). Mino ( $P < 0.01$ ), SB203580 ( $P < 0.01$ ) and STA-5326 ( $P < 0.01$ ) treatment significantly reversed these abnormalities.

### 3.10. CUMS-reduced hippocampal bcl-2/bax ratio was reversed by Mino, SB203580 or STA-5326

There was a significant interaction between CUMS and treatments in Bcl-2/Bax ratio ( $F_{3,42} = 3.46$ ,  $P < 0.05$ ) in the hippocampus. There was also a significant main effect of CUMS ( $F_{1,42} = 9.722$ ,  $P < 0.01$ ) and treatments ( $F_{3,42} = 3.546$ ,  $P < 0.05$ ) in hippocampal Bcl-2 concentration (Fig. 9B). The *post hoc* test revealed CUMS significantly down-regulated Bcl-2/Bax ratio ( $P < 0.01$ ) in the hippocampus, and Mino ( $P < 0.01$ ), SB203580 ( $P < 0.01$ ) and STA-5326 ( $P < 0.01$ ) treatment significantly reversed this effect (Fig. 9C).

### 3.11. Correlations between neuroinflammation/neurotransmitters and anhedonia behaviors

There was a negative correlation between sucrose preference and

hippocampal p-p38 concentration ( $r = -0.3241$ ,  $P < 0.05$ ) (Fig. 10C). Additionally, we found a positive correlation between sucrose preference and PFC neurotransmitters (5-HT/5-HIAA:  $r = 0.2957$ ,  $P < 0.05$ ; NE:  $r = 0.3973$ ,  $P < 0.01$ ) (Fig. 10D and E).

### 3.12. Correlations between neuroinflammation/neurotransmitters and anxiety behaviors

There was a negative correlation between Open T and hippocampal IL-12 concentration ( $r = -0.4283$ ,  $P < 0.01$ ) (Fig. 11AD), and a negative correlation between Open T and hippocampal Iba-1 concentration ( $r = -0.3314$ ,  $P < 0.05$ ) (Fig. 11B). Additionally, we found a positive correlation between Open T and PFC neurotransmitters (5-HT/5-HIAA:  $r = 0.2957$ ,  $P < 0.05$ ; NE:  $r = 0.3973$ ,  $P < 0.01$ ) (Fig. 11D and E).

### 3.13. Spearman correlations between hippocampal Iba-1 or IL-12 and p-p38, between IFN- $\gamma$ /IL-4 ratio and p-p38

There were positive correlations between hippocampal IL-12 and p-p38 ( $r = 0.2822$ ,  $P < 0.05$ ) (Fig. 12A); between hippocampal p-p38 and Iba-1 ( $r = 0.3629$ ,  $P < 0.01$ ) (Fig. 12B); between hippocampal IFN- $\gamma$ /IL-4 ratio and p-p38 ( $r = 0.5086$ ,  $P < 0.01$ ) (Fig. 12C); between hippocampal IL-12 and Iba-1 ( $r = 0.7435$ ,  $P < 0.01$ ) (Fig. 12D).

## 4. Discussion

This study systematically investigated lymphocyte subtype and neuroinflammatory alterations in chronic stress. Inhibiting Th1 lymphocytes, M1 microglia, or p38-MAPK pathway all alleviated depression-like behaviors, accompanied by suppressed neuroinflammatory signaling and restored neuroplasticity. Moreover, the

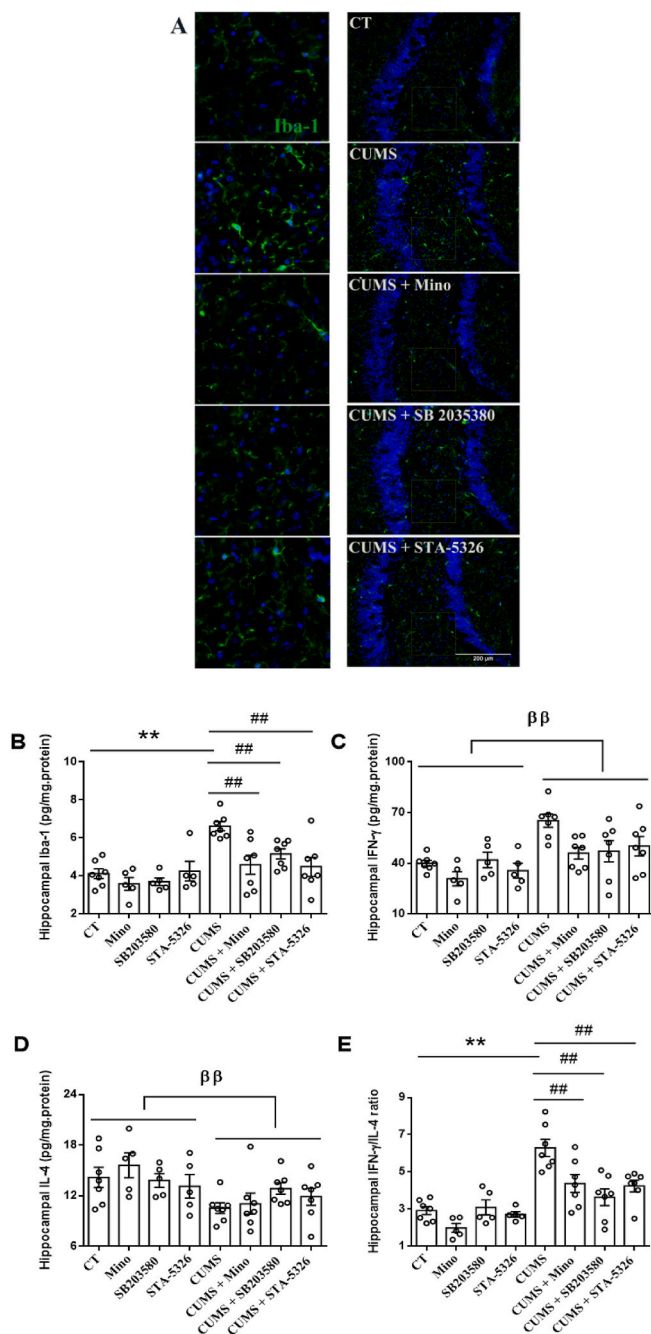


**Fig. 7.** Mino, SB203580 or STA-5326 reversed CUMS-induced microglia activation and the imbalance between Th1 and Th2 cytokines in the hippocampus. A) Representative photomicrographs of Iba-1 immunopositive cells in the dentate gyrus. Scale bar denotes 200  $\mu$ m, magnification 20 $\times$ ; B) Iba-1 concentration in the hippocampus; C) IFN- $\gamma$  concentration in the hippocampus; D) IL-4 concentration in the hippocampus; E) Hippocampal IFN- $\gamma$ /IL-4 ratio. All data are expressed as the mean  $\pm$  SEM. N = 5 for Mino, SB203580 and STA-5326 groups, N = 7 for remaining groups.  $^{\beta\beta}P < 0.01$  CUMS main effect.  $^{**}P < 0.01$  CUMS vs. control;  $^{\#}P < 0.05$ ,  $^{##}P < 0.01$  vs. CUMS.

present study is the first time to find that Th1 inhibition STA-5326 showed greater efficacy in restoring anhedonia and meningeal CD4 T cell levels, while SB203580 was most effective in normalizing 5-HT system. These findings are discussed below.

#### 4.1. CUMS-induced abnormal changes in peripheral and central lymphocyte and microglia subtypes

The present study found that CUMS reduced peripheral CD4/CD8 and Th2/Th1 ratios in the spleen and thymus, reflecting an activation of inflammatory response. Previous studies have reported that chronic stress activated peripheral macrophages/lymphocytes and promoted the differentiation of naive CD4 T cells to Th1 and Th17 cells. These changes increased peripheral Th1/Th2 and IL-17/Treg cells ratios, leading to an increase in pro-inflammatory cytokines, such as IFN- $\gamma$ , IL-1 $\beta$ , IL-6 and IL-17 (Hong et al., 2013; Zhao et al., 2015). More importantly, the present study for the first time found that CUMS significantly reduced meningeal CD4 lymphocyte subtypes, which was associated with increased hippocampal M1-microglia Iba-1 expression and Th1/Th2 (IFN- $\gamma$ /IL-4) ratio. The changes in the central lymphocyte subtypes may result from three aspects.

First, chronic stress exposure damages the blood-brain barrier (BBB), allowing peripheral immune cells such as macrophages and T lymphocytes to cross the BBB into the brain and interact with microglia (Alves de Lima et al., 2020; Engelhardt et al., 2017; Menard et al., 2017; Pasciuto et al., 2020b; Sántha et al., 2015; Scheinert et al., 2016; Weber et al., 2017). Second, lymphocytes in the meningeal vessels, located along dural sinuses, circulate in the cerebrospinal fluid (CSF) through the brain, and then migrate via these vessels to the deep cervical lymph nodes. This lymphatic pathway connects the CNS with peripheral immune system and plays a key role in regulating neuroinflammation (Louveau et al., 2015). Third, brain inherent T lymphocytes have recently been found at steady state, which gather in the subformal organ (Yoshida and Nguyen, 2025). These lymphocytes regulate microglial function via cytokine signaling (e.g., IFN- $\gamma$ , IL-4, IL-10) during CNS injury and disease. For example, Tregs suppress M1 microglial activation and neuroinflammation, whereas Th1 cells promote it (Greenhalgh et al., 2020). However, under stress conditions, the dynamics of these T cells and their potential interact with or impact on glial cells require further investigation.

Studies have demonstrated that brain CD4 cells are fundamental for microglial maturation and the absence of brain CD4 cells leads to reduced expression key synaptic pruning genes (AP-1, Egr1, and Lamp1) (Pasciuto et al., 2020a). Furthermore, CD4 T cells could regulate microglia polarization through activating inflammatory signaling, such as NF- $\kappa$ B pathway (Strachan-Whaley et al., 2014; H. Zhao et al., 2018), which subsequently affect Th1 and Th2 produced cytokines, such as IL-2, IFN- $\gamma$ , IL-4 (Aloisi et al., 1998; González and Pacheco, 2014). Meningeal T lymphocytes, particularly these IL-4 producing CD4 cells (Th2 cells), suppress the expression of proinflammatory cytokines (e.g., TNF, IL-12) in meningeal myeloid cells (microglia/macrophages), shifting them toward an anti-inflammatory phenotype. Depletion of these T cells or IL-4 deficiency leads to a proinflammatory skew in myeloid cells, reduced BDNF expression, and impaired learning and memory, highlighting a critical immune-brain interaction in behavior regulation (Derecki et al., 2010). Additionally, study demonstrates that central CD4 T cells accumulate in the meninges during the resolution of inflammation-induced depression. These cells promote the production of IL-10 in the meninges and prefrontal cortex, which suppress microglial activation and down-regulates IDO1 expression. By inhibiting proinflammatory cytokine signaling (e.g., IFN- $\gamma$ ) in microglia, IL-10 reduces kynurenine pathway activity, thereby resolving depression-like behavior (Laumet et al., 2018). Moreover, central CD4 T cells, particularly pathogenic Th17 cells, infiltrate the hippocampus during stress, expressing markers like CCR6 and IL-23R. These Th17 cells promote neuroinflammation by disrupting the blood-brain barrier and interacting with microglia, leading to depressive-like behaviors (Beurel et al., 2018). Our previous study has reported that CUMS induced the imbalance between T-cell subsets (e.g., Th17/Treg) through IL-2/IL-17 signaling and IL-6/TGF- $\beta$  pathway, thereby increasing pro-inflammatory phenotypes of microglia, and causing depression-like

**Table 2**  
Neurotransmitters and metabolism abnormalities in the hippocampus and PFC.

Neurotransmitters (ng/mg)		NE	DA	MHPG	5-HT	5-HIAA	NE/MHPG	5-HT/5-HIAA
Hippocampus	CT	12.49 ± 0.52	3.12 ± 0.08	0.76 ± 0.12	1.27 ± 0.07	0.53 ± 0.05	19.33 ± 3.66	2.54 ± 0.31
	Mino	13 ± 0.57	3.32 ± 0.04	0.76 ± 0.02	1.21 ± 0.05	0.51 ± 0.03	17.14 ± 0.98	2.43 ± 0.21
	SB203580	12 ± 0.68	3.01 ± 0.05	0.83 ± 0.18	1.2 ± 0.11	0.58 ± 0.06	17.11 ± 3.17	2.08 ± 0.11
	STA-5326	12.8 ± 0.82	2.99 ± 0.09	0.88 ± 0.07	1.11 ± 0.05	0.56 ± 0.04	14.93 ± 1.5	2.02 ± 0.08
	CUMS	9.47 ± 0.5**	2.72 ± 0.13**	0.86 ± 0.03	0.92 ± 0.04**	0.55 ± 0.03	11.05 ± 0.75	1.67 ± 0.06**
	CUMS + Mino	12.72 ± 0.5##	3.01 ± 0.12#	0.88 ± 0.1	1.11 ± 0.05	0.56 ± 0.04	15.41 ± 1.86	2.03 ± 0.11
	CUMS + SB203580	11.56 ± 0.53#	2.96 ± 0.1	1.02 ± 0.11	1.43 ± 0.12##,α,γγ	0.56 ± 0.06	11.95 ± 1.33	2.6 ± 0.1##,γ
	CUMS + STA-5326	12.33 ± 0.46#	3.13 ± 0.08##	0.76 ± 0.07	1.19 ± 0.07#	0.51 ± 0.03	17.21 ± 2.34	2.4 ± 0.23##
PFC	CT	10.57 ± 0.48	2.84 ± 0.1	0.69 ± 0.12	1.05 ± 0.04	0.37 ± 0.03	20.58 ± 6.57	2.93 ± 0.28
	Mino	11.27 ± 0.79	3.01 ± 0.15	0.53 ± 0.06	1.07 ± 0.07	0.43 ± 0.05	21.74 ± 2.31	2.53 ± 0.14
	SB203580	10.27 ± 0.37	2.66 ± 0.11	0.42 ± 0.12	1.07 ± 0.16	0.37 ± 0.04	39.76 ± 15.07	2.98 ± 0.48
	STA-5326	10.93 ± 1.16	2.79 ± 0.16	0.55 ± 0.05	1.01 ± 0.07	0.43 ± 0.02	20.21 ± 1.78	2.38 ± 0.12
	CUMS	8.93 ± 0.25*	2.79 ± 0.14	0.61 ± 0.05	0.83 ± 0.04*	0.43 ± 0.01	14.92 ± 0.87	1.94 ± 0.08**
	CUMS + Mino	11.23 ± 0.53#	2.75 ± 0.25	0.56 ± 0.04	1 ± 0.05	0.43 ± 0.03	20.43 ± 1.56	2.36 ± 0.13
	CUMS + SB203580	10.43 ± 1.04#	2.74 ± 0.26	0.57 ± 0.13	1.17 ± 0.09#	0.36 ± 0.03	24.29 ± 5.52	3.36 ± 0.31##,α,γγ
	CUMS + STA-5326	10.79 ± 0.34#	3.01 ± 0.09	0.45 ± 0.05	1.11 ± 0.06#	0.46 ± 0.03	25.93 ± 3.33	2.47 ± 0.18

All data are expressed as the mean ± SEM (n = 5-6 per group). <sup>β</sup>P < 0.05 CUMS main effect. \*P < 0.05, \*\*P < 0.01 CUMS vs. control; #P < 0.05, ##P < 0.01 vs. CUMS; <sup>γ</sup>P < 0.05 CUMS + SB203580 vs. CUMS + Mino; <sup>α</sup>P < 0.05 CUMS + SB203580 vs. CUMS + STA-5326.

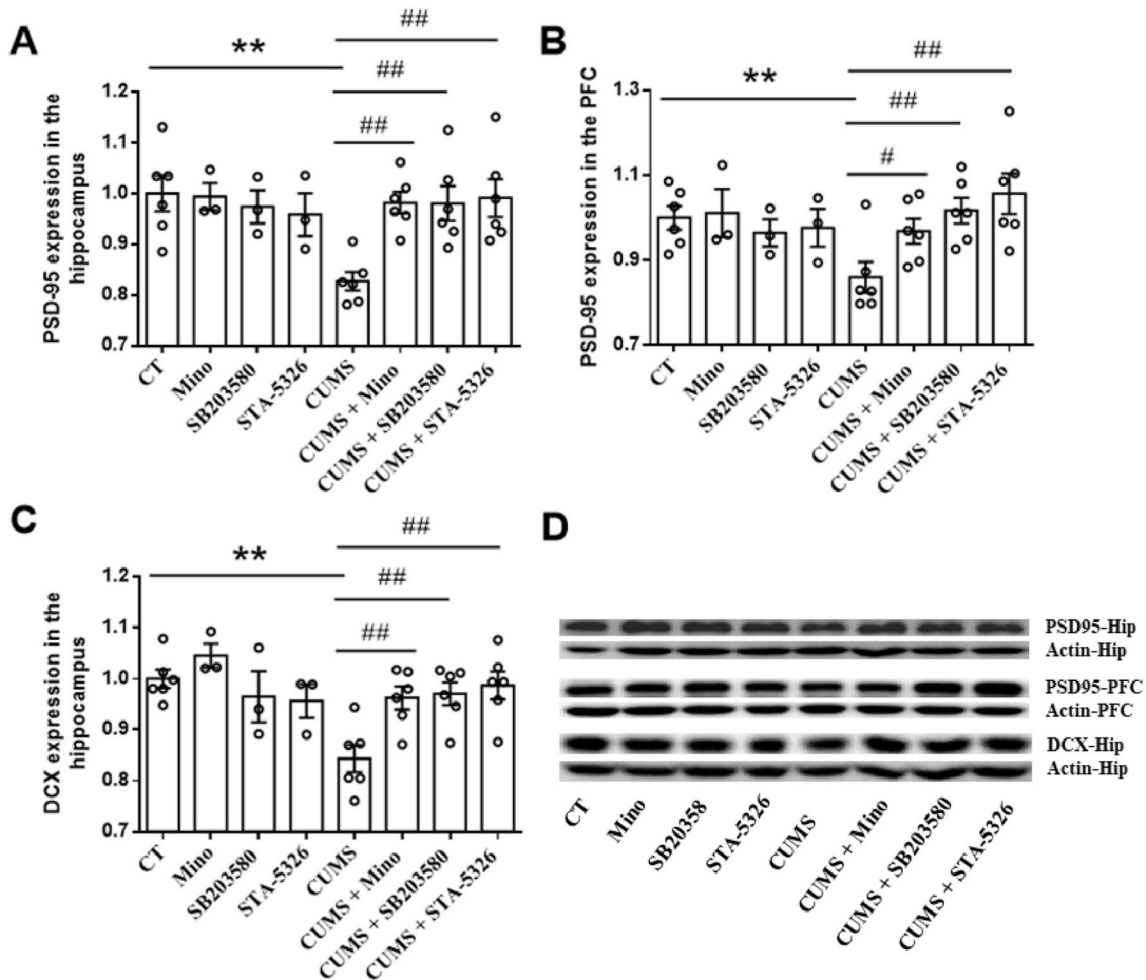


**Fig. 8.** Mino, SB203580 or STA-5326 reversed CUMS-induced decrease of PSD-95 and DCX expression. A) PSD-95 expression in the hippocampus; B) PSD-95 expression in the PFC; C) DCX expression in the hippocampus; D) WB band of PSD-95 and DCX expression. All data are expressed as the mean ± SEM. N = 3 for Mino, SB203580 and STA-5326 groups, N = 6 for remaining groups. \*\*P < 0.01 CUMS vs. control; #P < 0.05, ##P < 0.01 vs. CUMS.

changes (Huang et al., 2022). Taking together with our findings, the present study suggests that the imbalance between peripheral CD4/CD8 and Th1/Th2 lymphocytes, reduction of central CD4 lymphocyte and activation of M1-microglia phenotype after CUMS may increase central

pro-inflammatory cytokines and induce depression-like behaviors.

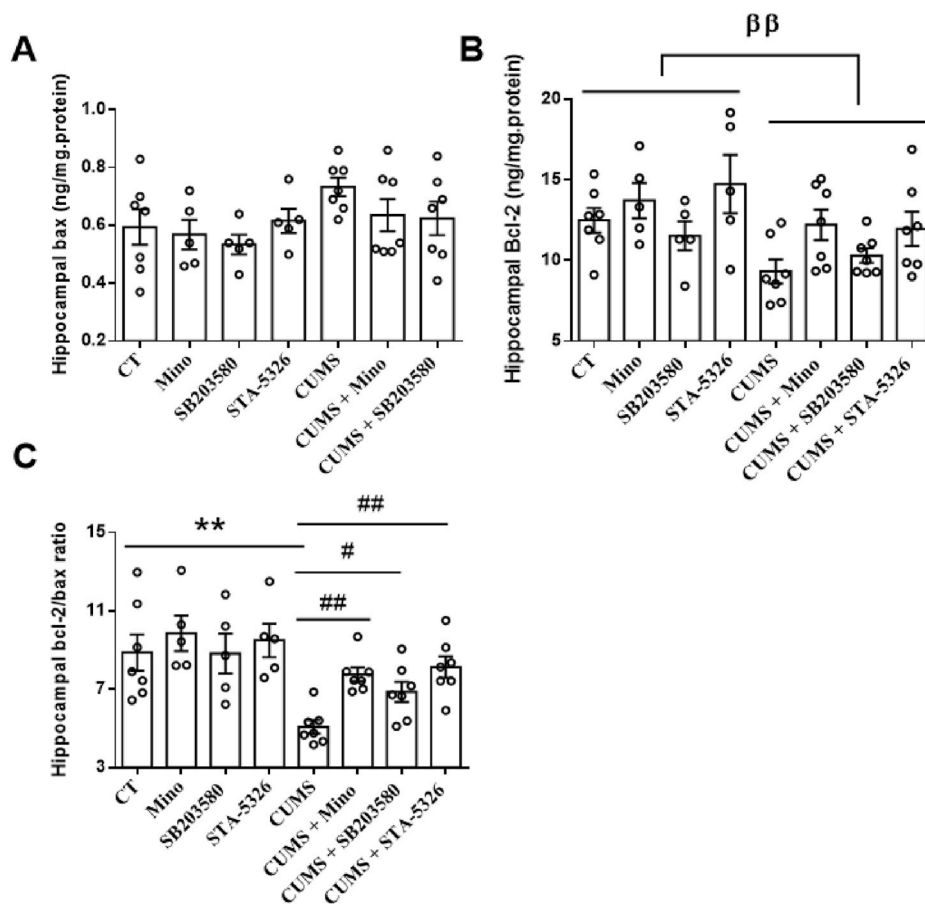


Fig. 9. Mino, SB203580 or STA-5326 reversed CUMS-induced apoptosis in the hippocampus. A) Bax concentration in the hippocampus. B) Bcl-2 concentration in the hippocampus. C) Bcl-2/Bax ratio in the hippocampus. All data are expressed as the mean  $\pm$  SEM. N = 5 for Mino, SB203580 and STA-5326 groups, N = 7 for remaining groups.  $\beta\beta P < 0.01$  CUMS main effect. \*\* $P < 0.01$  CUMS vs. control; # $P < 0.05$ , ## $P < 0.01$  vs. CUMS.

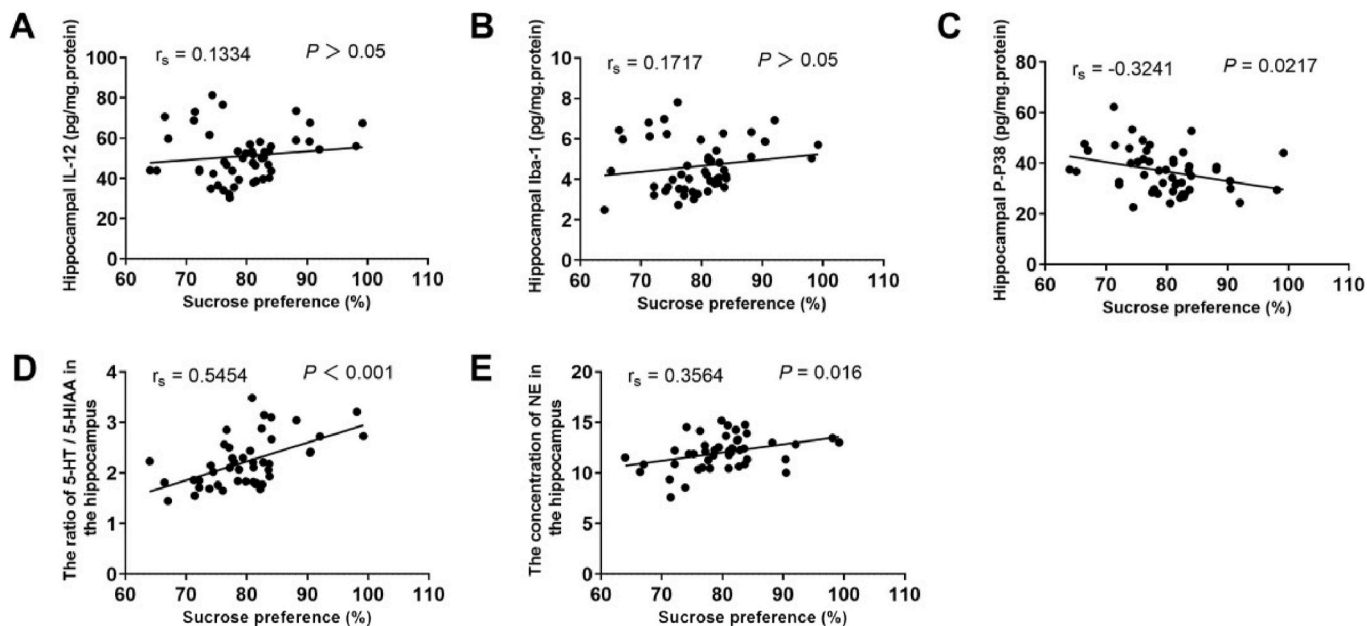


Fig. 10. Spearman correlations between neuroinflammation/neurotransmitters and anhedonia behaviors. A) Correlation between sucrose preference and hippocampal IL-12; B) Correlation between sucrose preference and hippocampal Iba-1; C) Correlations between sucrose preference and hippocampal p-p38; D) Correlation between sucrose preference and hippocampal 5-HT/5-HIAA ratio; E) Correlation between sucrose preference and hippocampal NE.

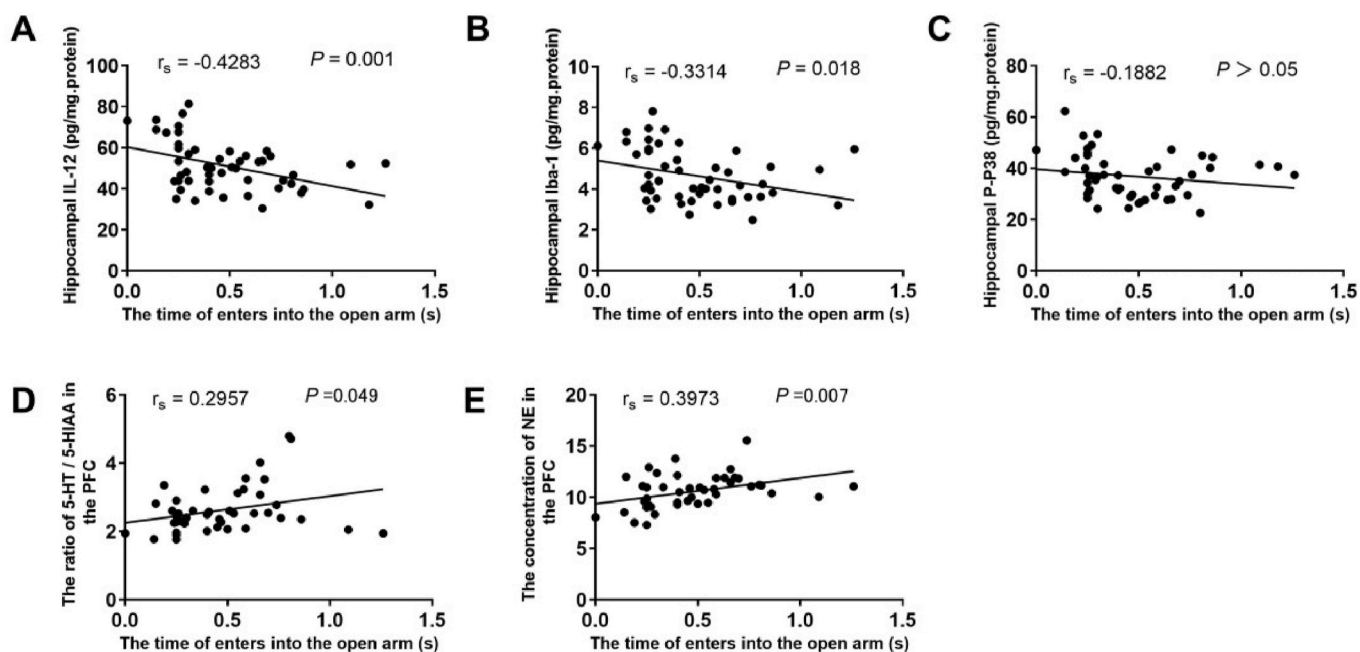


Fig. 11. Spearman correlations between neuroinflammation/neurotransmitters and anxiety behaviors. A) Correlation between Open T and hippocampal IL-12; B) Correlation between Open T and hippocampal Iba-1; C) Correlation between Open T and hippocampal p-p38; D) Correlation between Open T and PFC 5-HT/5-HIAA ratio; E) Correlation between Open T and PFC NE.

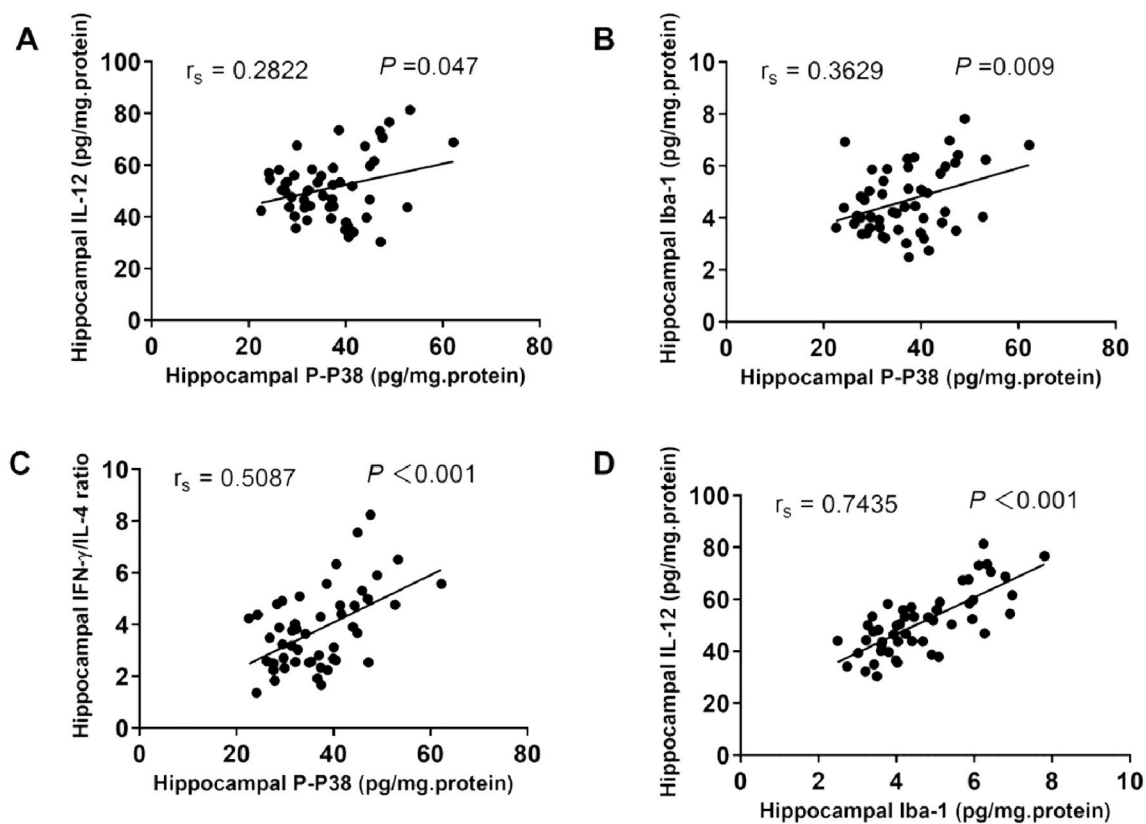


Fig. 12. Spearman correlations between hippocampal Iba-1 or IL-12 and p-p38, between IFN- $\gamma$ /IL-4 ratio and p-p38. A) Correlations between hippocampal IL-12 and p-p38; B) Correlations between hippocampal p-p38 and Iba-1; C) Correlations between hippocampal IFN- $\gamma$ /IL-4 ratio and p-p38; D) Correlations between hippocampal IL-12 and Iba-1.

#### 4.2. The potential relationship between Th1-lymphocytes or microglia and p38 pathway

Previous study has reported that a total of 2106 genes were differentially regulated in microglia in response to Th1-derived factors (Prajeeth et al., 2018). Furthermore, Th1-associated factors, but not Th2 and Th17 cells, that infiltrate the CNS can stimulate resident microglia to directly trigger proinflammatory M1-type gene expression (Prajeeth et al., 2017; Séguin et al., 2003). Thus, the present study, by using STA-5326 to target Th1 lymphocytes, for the first time showed that the treatment inhibited hippocampal microglia Iba-1 expression and p38-MAPK pro-inflammatory pathway, thereby balanced central Th1 and Th2 cytokines in the CUMS model.

To further investigate the potential relationship between Th1 lymphocytes and microglia, Mino was administered to specifically target the M1 microglial phenotype. The results demonstrated that Mino significantly reversed CUMS-induced alterations in peripheral CD4/CD8 and Th1/Th2 ratios, increased the proportion of central CD4 T lymphocytes, and inhibited the pro-inflammatory p38-MAPK signaling pathway. Consequently, Mino normalized hippocampal levels of Th1-associated cytokines (IL-2, IL-12, IFN- $\gamma$ ) and the Th2 cytokine IL-4. A previous study reported that microglia from experimental autoimmune encephalomyelitis mice inhibited the proliferation of antigen-specific CD4 T cells, but promoted the differentiation of Th1 cells through nitric oxide (NO) pathway (Hu et al., 2016). Additionally, treatment of microglia with glucocorticoids reduced their ability to stimulate CD4 cell proliferation, which induced a shift from Th1 to the Th2 response (Li et al., 2007).

To demonstrate the involvement of p38-MAPK pathway in CUMS-induced neuroinflammation, the present study inhibited the pathway using the p38-MAPK inhibitor SB203580. SB203580 markedly normalized CUMS-induced alterations in Th1-lymphocyte and M1-microglial subtypes, and restored the balance between hippocampal Th1 and Th2 cytokines. A previous study has demonstrated that p38-MAPK was rapidly activated in effector Th1 cells, which required for transcription mediated by the IFN- $\gamma$  promoter. Conversely, the inhibition of p38-MAPK in CD4 T cells in the dnp38 transgenic mice resulted in decreased IFN- $\gamma$  production by Th1 cells (Rincón et al., 1998). Furthermore, another p38-MAPK inhibitor NJK14047 suppressed microglial cell activation and reduced the secretion of pro-inflammatory cytokines (TNF- $\alpha$ , IL-1 $\beta$  and IL-6) in BV2 microglia cells (M. S. Gee et al., 2018). More importantly, this study found hippocampal Iba-1, p-p38 and IL-12 levels were positively correlated with each other, and p-p38 was additionally correlated with a higher IFN- $\gamma$ /IL-4 ratio. These mean that there was a close interaction between the lymphocyte subtypes and microglia, which may regulate central Th1 and Th2 cytokine production via p38-MAPK inflammatory pathway in the CUMS model.

#### 4.3. The inhibition of Th1-lymphocytes, M1-microglia or p38-MAPK improved CUMS-induced deficiency of CORT, neurotransmitters and reduced neuroplasticity

Hyperactivity of the HPA axis is a well-established neuroendocrine feature of depression, characterized by elevated levels of CRH, ACTH, and cortisol in the cerebrospinal fluid of affected individuals (Nemeroff et al., 1984). Previous work demonstrated that CUMS significantly increased CORT levels in serum or hippocampus (Peng et al., 2020; Wang et al., 2025; Zhang et al., 2019a,b). The present study further demonstrated that stress-increased CORT could be reduced by three treatments. The mechanism may relate to the normalization of the interaction between CORT and neuroinflammation (Xu et al., 2025). Furthermore, we found strong correlations between hippocampal neurotransmitters and anhedonia, as well as a correlation between anxiety and PFC neurotransmitters. More importantly, the present study for the first found that inhibition of Th1 cells with STA-5326, targeting of M1 microglia with minocycline, or blockade of the p38-MAPK pathway with

SB203580 significantly ameliorated CUMS-induced neurotransmitter dysfunctions in the prefrontal cortex and hippocampus, which were associated with reversed depression-like behaviors. Chronic microglial activation up-regulates indoleamine 2,3-dioxygenase (IDO) expression, depleting tryptophan and thus reducing serotonin (5-HT) synthesis. Concurrently, the released proinflammatory cytokines enhance monoamine oxidase (MAO) activity, accelerating the degradation of neurotransmitters such as norepinephrine (NE) and dopamine (DA) (Kong et al., 2026; A. H. Miller et al., 2009; Shih et al., 1999). Meanwhile, IFN- $\gamma$  derived from Th1 cells not only drives microglia polarization towards the pro-inflammatory M1 phenotype but also further activates IDO, creating an inflammatory amplification loop (Bai et al., 2024; Kwizdzinski and Bechmann, 2007). Furthermore, p38 MAPK, a key molecule of the inflammatory pathway, has been proven to up-regulate the expression and activity of the membrane transporter for 5-HT, NE, and DA, thereby increase the clearance rate of 5-HT, NE, and DA in the synaptic cleft (Baganz et al., 2015; A. H. Miller et al., 2009). Thus, microglial inhibitors, Th1 inhibitors, and p38 MAPK inhibitors can restore concentration of neurotransmitters such as 5-HT and NE by modulating neuroinflammatory pathways, thereby improving depressive-like behaviors.

With regard to the reduction of neuroplasticity in depression, the present study found that doublecortin (DCX) and PSD-95, two classical markers of respectively synaptic plasticity and neurogenesis, were decreased in the hippocampus and PFC of CUMS mouse brains. It is well known that the reduction of neurogenesis and synaptic plasticity are the contributor to neuronal apoptosis and depressive behaviors (Joëls et al., 2004; M. Kubera et al., 2011). The present study further showed that CUMS-reduced anti-apoptotic factor Bcl-2 and Bcl-2/Bax ratio in the hippocampus, which was significantly reversed by STA-5326, Mino or SB203580 treatment.

STA-5326 is a selective Th1 immunosuppressant, with powerful inhibition on Th1 cytokines IFN- $\gamma$  and IL-12 (Langrish et al., 2004; Wada et al., 2007). This study demonstrated STA-5326 treatment shifted hippocampal Th1 to Th2 phenotype (decreased IL-2 and IFN- $\gamma$ /IL-4) and increased central CD4 lymphocytes while increasing DCX, PSD-95 and Bcl-2/Bax ratio in the hippocampus or PFC. It was found that remodeling Th1 (IFN- $\gamma$ , IL-6) and Th2 (IL-4, IL-10) polarized environment could increase hippocampal neurogenesis in stressed mice (Palumbo et al., 2010, 2012). For instance, M1 microglia (CD68) was activated by Th1 cytokine IFN- $\gamma$ -injection, which increased pro-inflammatory cytokines (IL-1 $\beta$ , TNF- $\alpha$ , IL-6) and nitric oxide (NO) release. These changes were associated with the reduction of long-term adult hippocampal neurogenesis (DCX and BrdU) (Zhang et al., 2020). In addition, hippocampal neurogenesis was increased in IL-2 KO mice (Beck et al., 2005). On the other hand, absence of CD4 T cells resulted in defective synaptic pruning, while systemic depletion of CD4 positive T lymphocytes led to significantly reduced hippocampal neurogenesis (Pasciuto et al., 2020b; Wolf et al., 2009; Zarif et al., 2018). However, adoptive transfer of CD4 T lymphocytes into Rag1<sup>-/-</sup> mice promoted the proliferation of hippocampal neurons and improved learning and anxiety-like behaviors (Rattazzi et al., 2013; Wolf et al., 2009; Ziv et al., 2006). Therefore, the present study demonstrated that selective inhibited Th1 lymphocyte increased hippocampal neuroplasticity in stressed mice through balancing hippocampal Th1 and Th2 cytokines.

Another key finding of this study was that Mino normalized CUMS-induced alterations in neuroplasticity, as evidenced by increasing PSD-95, DCX and bcl-2/bax ratio. A previous study is in line with our results by demonstrating that Mino promotes dendritic spine formation in the hippocampal CA1 and DG and improves cognitive function by up-regulating PSD-95 in aged mice (Jiang et al., 2015). Additionally, Mino alleviates stress-induced depression-like behaviors by restoring neurogenesis (DCX/BrdU), likely through suppressing M1 microglial polarization (reducing CD68 and Iba-1/Arg1 ratio) in hippocampal subregions (DG, CA1, CA2), which subsequently decreases IL-1 $\beta$  and IL-6, while increasing IL-4 level (Bassett et al., 2021; Han et al., 2019).

Such anti-inflammatory function benefited neuronal proliferation, differentiation, and survival (Borsini et al., 2015; Roque et al., 2016). Moreover, Mino can up-regulate Bcl-2 level and protect against cell death in mitochondria (Wang et al., 2004). These findings support that Mino treatment reversed depression-like behaviors through attenuating CUMS-induced neuroplasticity degeneration.

Furthermore, the present study showed that SB203580 treatment increased PSD-95, DCX and bcl-2/bax ratio in the CUMS model. Pro-inflammatory cytokines, such as IL-1 $\beta$ , TNF- $\alpha$  have been reported to affect neuronal synaptic functioning via p38-MAPK signaling in a variety of brain regions (Falcicchia et al., 2020), and SB203580 can increase hippocampal PSD-95 and improves cognitive impairment by inhibiting p38-MAPK activation (Ye et al., 2020). An in vitro study reported that SB203580 can reverse lipopolysaccharide-induced apoptosis by restoring Bax and Bcl2 expressions (Xiong et al., 2019). SB203580 treatment decreased Iba-1-positive microglia expression, and pro-inflammatory IL-1 $\beta$ , IL-6 and IFN- $\gamma$  concentrations, and increased anti-inflammatory IL-4 and IL-10 factors, which attenuated neuronal dysfunction and improved depression-like behaviors in miR-26a-3p deficiency mouse (Wang et al., 2022). Moreover, a strong correlation between anhedonia and hippocampal p-p38 was found in this study. Thus, the present study revealed that SB203580 treatment increased neuroplasticity and improved depression-like behaviors through inhibiting p38-MAPK signal in CUMS model.

#### 4.4. Different efficacy of three inhibitors in the modulation of behaviors and relevant molecular markers

First, the study found that STA-5326 and SB203580 presented better effects on the reduction of thymic Th1/Th2 ratio compared to Mino after CUMS. STA-5326 has been used in the treatment of Th1-related autoimmune or immunologic disorders (Langrish et al., 2004; Wada et al., 2007). However, Mino selectively inhibits M1 polarization of microglia/macrophages, and decreases M1 pro-inflammatory factors, which was widely used in inflammatory disease (Kobayashi et al., 2013). Additionally, the p38-MAPK is required for Th1 immune responses by regulating the production of IFN- $\gamma$  and IL-12 in CD4 T cells, and is the most important for IL-2R signaling in primary T-lymphocytes (Conrad et al., 2009; Nguyen et al., 2000; Rincón et al., 1998; S. Zhang and Kaplan, 2000). These mechanisms of action might explain why SB203580 presented better effects than Mino on regulating thymic Th1 and Th2 lymphocytes.

Second, STA-5326 was more potent than Mino and SB203580 in increasing central CD4 lymphocyte subtypes and normalizing anhedonia behavior, while its effect on anxious behavior was similar to other two inhibitors. STA-5326 was reported to be able to selectively suppress naive CD4 cell differentiation into Th1 lymphocyte subtypes (K. Gee et al., 2009; Langrish et al., 2004), leading to the inhibitions of pro-inflammatory factor productions, especially in IL-12 and IFN- $\gamma$  cytokines (Sun et al., 2015). These data may provide an explanation for present findings that STA-5326 was more efficient than SB203580 and Mino to restore the number of CD4 cells. STA-5326 was shown to be more effective in anhedonia improvement, which maybe from its increase in dopamine concentration in both the hippocampus and PFC (Nestler and Carlezon, 2006). Evidence from a clinical trial showed that anti-IL-12 antibody ustekinumab (similar as STA-5326) treatment was more powerful than anti-P38/MAPK (losmapimod), anti-TNF- $\alpha$  (infliximab or golimumab) or anti-COX-2 (GW406381) in the treatment of major depressive patients (Wittenberg et al., 2020). However, The comparable improvement in anxiety-like behaviors observed across all three inhibitors may be attributed to their similar capacity to modulate neuroinflammation, neuroplasticity, and apoptosis, pathways that are critically involved in the regulation of anxiety (Salim et al., 2012; Sha and Xu, 2023).

Third, the present study found that the inhibition of p38-MAPK inflammatory pathway by SB203580 was more efficient than Mino and

STA-5326 in restoring 5-HT/5-HIAA ratio in both the hippocampus and PFC of CUMS mice. It is well known that inflammatory response- or CUMS-induced pro-inflammatory cytokines can activate indoleamine 2, 3-dioxygenase (IDO) via p38-MAPK (Fujigaki et al., 2006). This activation of the IDO enzyme leads to the degradation of tryptophan consequently affecting 5-HT synthesis and triggering depression-like behaviors (Miura et al., 2008). Similar result was found after p38-MAPK inhibitor SB202190 treatment, which could significantly inhibit IDO expression (Fu et al., 2011), and decreased 5-HT turnover and improved depression-like behaviors (Zhu et al., 2010). These data indicate that p38-MAPK pathway is the indispensability in 5-HT synthesis and re-uptake. Thus, SB203580 may be more potent in regulating 5-HT synthesis and metabolism than Mino and STA-5326.

## 5. Conclusion

Overall, this study systemically demonstrated the pathway of peripheral immune cells-microglial activation-neuroinflammation-neuroplasticity-depressive behaviors by pharmacological interventions targeting Th1 lymphocytes (STA-5326), M1 microglia (Mino), or the p38-MAPK pathway (SB203580). Among the three treatments, STA-5326 showed superior efficacy in mitigating anhedonia, and restoring thymic Th1/Th2 ratio and meningeal CD4 T cell levels, whereas SB203580 was most effective in normalizing serotonergic system.

There are some limitations in the present study. Firstly, different drug doses and other brain regions, such as CA1, CA3, DG, dorsal or ventral in the hippocampus should be studied in the future study. Secondly, more detailed peripheral and central lymphocyte subtypes should be evaluated, such as Th1/Th2, Th17/Treg cells, etc. Third, an in vitro cellular experiment should be added, which allows us to directly assess cytokines secreted from different lymphocyte subtypes. Fourth, Th1 lymphocytes, microglia or p38-MAPK knockdown mice might be used to further demonstrate the relationship between Th1 lymphocytes and microglia. Fifth, other depression-related behaviors should be tested, which explore the different efficacy of three treatments, such as helplessness, memory, or locomotion activity, etc. Finally, given that the prevalence of depression is higher in females than in males in clinical patients, future studies should include both male and female animals.

## CRediT authorship contribution statement

**Cai Zhang:** Writing – original draft, Conceptualization. **Baiping Liu:** Writing – review & editing. **Xiaohong Li:** Writing – review & editing. **Thierry D. Charlier:** Writing – review & editing, Supervision. **Kirthana Kunikullaya U:** Writing – review & editing. **HarryW.M. Steinbusch:** Writing – review & editing, Supervision. **Cai Song:** Writing – review & editing, Supervision, Funding acquisition.

## Declaration of competing interest

The authors declare the following financial interests/personal relationships which may be considered as potential competing interests: Reports a relationship with that includes: Has patent pending to. If there are other authors, they declare that they have no known competing financial interests or personal relationships that could have appeared to influence the work reported in this paper.

## Acknowledgments

This work was supported by grants to CS from Province natural science fund of Guangdong (2021A1515011579), Shenzhen Science and technology plan (International Cooperation Research) project (GJHZ20190823111414825), Zhanjiang Science and Technology Project (2021A05046), Guangdong Science and Technology Project (2016B020235001).

## Appendix A. Supplementary data

Supplementary data to this article can be found online at <https://doi.org/10.1016/j.ejphar.2026.178710>.

## Data availability

Data will be made available on request.

## References

- Aloisi, F., Ria, F., Penna, G., Adorini, L., 1998. Microglia are more efficient than astrocytes in antigen processing and in Th1 but not Th2 cell activation. *J. Immunol.* 160 (10), 4671–4680.
- Alves de Lima, K., Rustenhoven, J., Kipnis, J., 2020. Meningeal immunity and its function in maintenance of the central nervous system in health and disease. *Annu. Rev. Immunol.* 38, 597–620. <https://doi.org/10.1146/annurev-immunol-102319-103410>.
- Baganz, N.L., Lindler, K.M., Zhu, C.B., Smith, J.T., Robson, M.J., Iwamoto, H., Deneris, E. S., Hewlett, W.A., Blakely, R.D., 2015. A requirement of serotonergic p38 $\alpha$  mitogen-activated protein kinase for peripheral immune system activation of CNS serotonin uptake and serotonin-linked behaviors. *Transl. Psychiatry* 5 (11), e671. <https://doi.org/10.1038/tp.2015.168>.
- Bai, Y., Cai, Y., Chang, D., Li, D., Huo, X., Zhu, T., 2024. Immunotherapy for depression: recent insights and future targets. *Pharmacol. Ther.* 257, 108624. <https://doi.org/10.1016/j.pharmthera.2024.108624>.
- Bassett, B., Subramaniam, S., Fan, Y., Varney, S., Pan, H., Carneiro, A.M.D., Chung, C. Y., 2021. Minocycline alleviates depression-like symptoms by rescuing decrease in neurogenesis in dorsal hippocampus via blocking microglia activation/phagocytosis. *Brain Behav. Immun.* 91, 519–530. <https://doi.org/10.1016/j.bbi.2020.11.009>.
- Beck Jr., R.D., Wasserfall, C., Ha, G.K., Cushman, J.D., Huang, Z., Atkinson, M.A., Pettito, J.M., 2005. Changes in hippocampal IL-15, related cytokines, and neurogenesis in IL-2 deficient mice. *Brain Res.* 1041 (2), 223–230. <https://doi.org/10.1016/j.brainres.2005.02.010>.
- Beurel, E., Lowell, J.A., Jope, R.S., 2018. Distinct characteristics of hippocampal pathogenic T(H)17 cells in a mouse model of depression. *Brain Behav. Immun.* 73, 180–191. <https://doi.org/10.1016/j.bbi.2018.04.012>.
- Borsini, A., Zunszain, P.A., Thuret, S., Pariante, C.M., 2015. The role of inflammatory cytokines as key modulators of neurogenesis. *Trends Neurosci.* 38 (3), 145–157. <https://doi.org/10.1016/j.tins.2014.12.006>.
- Conrad, D.M., Furlong, S.J., Doucette, C.D., Boudreau, R.T., Hoskin, D.W., 2009. Role of mitogen-activated protein kinases in Thy-1-induced T-lymphocyte activation. *Cell. Signal.* 21 (8), 1298–1307. <https://doi.org/10.1016/j.cellsig.2009.03.014>.
- Derecki, N.C., Cardani, A.N., Yang, C.H., Quinlins, K.M., Crihfield, A., Lynch, K.R., Kipnis, J., 2010. Regulation of learning and memory by meningeal immunity: a key role for IL-4. *J. Exp. Med.* 207 (5), 1067–1080. <https://doi.org/10.1084/jem.20091419>.
- Engelhardt, B., Vajkoczy, P., Weller, R., 2017. The movers and shapers in immune privilege of the CNS. *Nat. Immunol.* 18 (2), 123–131. <https://doi.org/10.1038/ni.3666>.
- Falciocchia, C., Tozzi, F., Arancio, O., Watterson, D.M., Origlia, N., 2020. Involvement of p38 MAPK in synaptic function and dysfunction. *Int. J. Mol. Sci.* 21 (16). <https://doi.org/10.3390/ijms21166524>.
- Fan, K., Li, Y., Wang, H., Mao, X., Guo, J., Wang, F., Huang, L., Li, Y., Ma, X., Gao, Z., et al., 2019. Stress-induced metabolic disorder in peripheral CD4 T cells leads to anxiety-like behavior. *Cell* 179 (4), e819. <https://doi.org/10.1016/j.cell.2019.10.001>, 864–879.
- Fu, X., Lawson, M.A., Kelley, K.W., Dantzer, R., 2011. HIV-1 tat activates indoleamine 2,3 dioxygenase in murine organotypic hippocampal slice cultures in a p38 mitogen-activated protein kinase-dependent manner. *J. Neuroinflammation* 8, 88. <https://doi.org/10.1186/1742-2094-8-88>.
- Fujigaki, H., Saito, K., Fujigaki, S., Takemura, M., Sudo, K., Ishiguro, H., Seishima, M., 2006. The signal transducer and activator of transcription 1 $\alpha$  and interferon regulatory factor 1 are not essential for the induction of indoleamine 2,3-dioxygenase by lipopolysaccharide: involvement of p38 mitogen-activated protein kinase and nuclear factor-kappaB pathways, and synergistic effect of several proinflammatory cytokines. *J. Biochem.* 139 (4), 655–662. <https://doi.org/10.1093/jb/mvj072>.
- Gee, K., Guzzo, C., Che Mat, N.F., Ma, W., Kumar, A., 2009. The IL-12 family of cytokines in infection, inflammation and autoimmune disorders. *Inflamm. Allergy - Drug Targets* 8 (1), 40–52. <https://doi.org/10.2174/187152809787582507>.
- Gee, M.S., Kim, S.W., Kim, N., Lee, S.J., Oh, M.S., Jin, H.K., Bae, J.S., Inn, K.S., Kim, N.J., Lee, J.K., 2018. A novel and selective p38 mitogen-activated protein kinase inhibitor attenuates LPS-induced neuroinflammation in BV2 microglia and a mouse model. *Neurochem. Res.* 43 (12), 2362–2371. <https://doi.org/10.1007/s11064-018-2661-1>.
- González, H., Pacheco, R., 2014. T-cell-mediated regulation of neuroinflammation involved in neurodegenerative diseases. *J. Neuroinflammation* 11, 201. <https://doi.org/10.1186/s12974-014-0201-8>.
- Greenhalgh, A.D., David, S., Bennett, F.C., 2020. Immune cell regulation of glia during CNS injury and disease, 21 (3), 139–152. <https://doi.org/10.1038/s41583-020-0263-9>.
- Gu, M., Li, Y., Tang, H., Zhang, C., Li, W., Zhang, Y., 2018. Endogenous omega (n)-3 fatty acids in Fat-1 mice attenuated depression-like behavior, imbalance between microglial M1 and M2 phenotypes, and dysfunction of neurotrophins induced by lipopolysaccharide administration, 10 (10). <https://doi.org/10.3390/nu10101351>.
- Han, Y., Zhang, L., Wang, Q., Zhang, D., Zhao, Q., Zhang, J., Xie, L., Liu, G., You, Z., 2019. Minocycline inhibits microglial activation and alleviates depressive-like behaviors in Male adolescent mice subjected to maternal separation. *Psychoneuroendocrinology* 107, 37–45. <https://doi.org/10.1016/j.psyneuen.2019.04.021>.
- Hong, M., Zheng, J., Ding, Z.Y., Chen, J.H., Yu, L., Niu, Y., Hua, Y.Q., Wang, L.L., 2013. Imbalance between Th17 and treg cells may play an important role in the development of chronic unpredictable mild stress-induced depression in mice. *Neuroimmunomodulation* 20 (1), 39–50. <https://doi.org/10.1159/000343100>.
- Hu, J., He, H., Yang, Z., Zhu, G., Kang, L., Jing, X., Lu, H., Song, W., Bai, B., Tang, H., 2016. Programmed death Ligand-1 on Microglia regulates Th1 differentiation via nitric oxide in experimental autoimmune encephalomyelitis. *Neurosci. Bull.* 32 (1), 70–82. <https://doi.org/10.1007/s12264-015-0010-9>.
- Huang, C., Zhang, F., Li, P., 2022. Low-Dose IL-2 attenuated depression-like behaviors and pathological changes through restoring the balances between IL-6 and TGF- $\beta$  and between Th17 and treg in a chronic stress-induced mouse model of depression, 23 (22). <https://doi.org/10.3390/ijms232213856>.
- Jiang, Y., Liu, Y., Zhu, C., Ma, X., Ma, L., Zhou, L., Huang, Q., Cen, L., Pi, R., Chen, X., 2015. Minocycline enhances hippocampal memory, neuroplasticity and synapse-associated proteins in aged C57 BL/6 mice. *Neurobiol. Learn. Mem.* 121, 20–29. <https://doi.org/10.1016/j.nlm.2015.03.003>.
- Joëls, M., Karst, H., Alfarez, D., Heine, V., Qin, Y., van Riel, E., Verkuyl, M., Lucassen, P., Krugers, H., 2004. Effects of chronic stress on structure and cell function in rat hippocampus and hypothalamus. *Stress* 7 (4), 221–231. <https://doi.org/10.1080/10253890500070005>.
- Kobayashi, K., Imagama, S., Ohgomori, T., Hirano, K., Uchimura, K., Sakamoto, K., Hirakawa, A., Takeuchi, H., Suzumura, A., Ishiguro, N., et al., 2013. Minocycline selectively inhibits M1 polarization of microglia. *Cell Death Dis.* 4 (3), e525. <https://doi.org/10.1038/cddis.2013.54>.
- Kong, S., Huang, Z., Fang, Y., 2026. Research Progress on the Biological Function and Homeostatic Disruption of Microglia in the Pathogenesis of Major Depressive Disorder. <https://doi.org/10.1007/s12264-025-01571-5>.
- Kubera, M., Obuchowicz, E., Goehler, L., Brzeszcz, J., Maes, M., 2011. In animal models, psychosocial stress-induced (neuro)inflammation, apoptosis and reduced neurogenesis are associated to the onset of depression. *Prog. Neuropsychopharmacol. Biol. Psychiatry* 35 (3), 744–759. <https://doi.org/10.1016/j.pnpbp.2010.08.026>.
- Kubera, M., Van Bockstaele, D., Maes, M., 1999. Leukocyte subsets in treatment-resistant major depression. *Pol. J. Pharmacol.* 51 (6), 547–549.
- Kwidzinski, E., Bechmann, I., 2007. IDO expression in the brain: a double-edged sword. *J. Mol. Med. (Berl.)* 85 (12), 1351–1359. <https://doi.org/10.1007/s00109-007-0229-7>.
- Langrish, C.L., McKenzie, B.S., Wilson, N.J., de Waal Malefyt, R., Kastelein, R.A., Cua, D. J., 2004. IL-12 and IL-23: master regulators of innate and adaptive immunity. *Immunol. Rev.* 202, 96–105. <https://doi.org/10.1111/j.0105-2896.2004.00214.x>.
- Laumet, G., Edralin, J.D., Chiang, A.C., Dantzer, R., Heijnen, C.J., 2018. Resolution of inflammation-induced depression requires T lymphocytes and endogenous brain interleukin-10 signaling, 43 (13), 2597–2605. <https://doi.org/10.1038/s41386-018-0154-1>.
- Leonard, B.E., 2001. The immune system, depression and the action of antidepressants. *Prog. Neuropsychopharmacol. Biol. Psychiatry* 25 (4), 767–780. [https://doi.org/10.1016/s0278-5846\(01\)00155-5](https://doi.org/10.1016/s0278-5846(01)00155-5).
- Li, M., Wang, Y., Guo, R., Bai, Y., Yu, Z., 2007. Glucocorticoids impair microglia ability to induce T cell proliferation and Th1 polarization. *Immunol. Lett.* 109 (2), 129–137. <https://doi.org/10.1016/j.imlet.2007.02.002>.
- Liu, C., Tan, Y., Li, D., Tang, S., Wen, X., Long, Y., Sun, H., Hong, H., Hu, M., 2020. Zileuton ameliorates depressive-like behaviors, hippocampal neuroinflammation, apoptosis and synapse dysfunction in mice exposed to chronic mild stress. *Int. Immunopharmacol.* 78, 105947. <https://doi.org/10.1016/j.intimp.2019.105947>.
- Louveau, A., Smirnov, I., Keyes, T.J., Eccles, J.D., Rouhani, S.J., Peske, J.D., Derecki, N. C., Castle, D., Mandell, J.W., Lee, K.S., et al., 2015. Structural and functional features of central nervous system lymphatic vessels. *Nature* 523 (7560), 337–341. <https://doi.org/10.1038/nature14432>.
- Maes, M., Smith, R., Scharpe, S., 1995. The monocyte-T-lymphocyte hypothesis of major depression. *Psychoneuroendocrinology* 20 (2), 111–116. [https://doi.org/10.1016/0306-4530\(94\)00066-j](https://doi.org/10.1016/0306-4530(94)00066-j).
- Menard, C., Pfau, M.L., Hodes, G.E., Kana, V., Wang, V.X., Bouchard, S., Takahashi, A., Flanigan, M.E., Aleyasin, H., LeClair, K.B., et al., 2017. Social stress induces neurovascular pathology promoting depression, 20 (12), 1752–1760. <https://doi.org/10.1038/s41593-017-0010-3>.
- Miller, A., 2010. Depression and immunity: a role for T cells? *Brain Behav. Immun.* 24 (1), 1–8. <https://doi.org/10.1016/j.bbi.2009.09.009>.
- Miller, A.H., Maletic, V., Raison, C.L., 2009. Inflammation and its discontents: the role of cytokines in the pathophysiology of major depression. *Biol. Psychiatry* 65 (9), 732–741. <https://doi.org/10.1016/j.biopsych.2008.11.029>.
- Miura, H., Ozaki, N., Sawada, M., Isobe, K., Ohta, T., Nagatsu, T., 2008. A link between stress and depression: shifts in the balance between the kynurenine and serotonin pathways of tryptophan metabolism and the etiology and pathophysiology of depression. *Stress* 11 (3), 198–209. <https://doi.org/10.1080/10253890701754068>.
- Morganti, J.M., Goulding, D.S., Van Eldik, L.J., 2019. Deletion of p38 $\alpha$  MAPK in microglia blunts trauma-induced inflammatory responses in mice. *J. Neuroinflammation* 16 (1), 98. <https://doi.org/10.1186/s12974-019-1493-5>.

- Myint, A.M., Leonard, B.E., Steinbusch, H.W., Kim, Y.K., 2005. Th1, Th2, and Th3 cytokine alterations in major depression. *J. Affect. Disord.* 88 (2), 167–173. <https://doi.org/10.1016/j.jad.2005.07.008>.
- Nemeroff, C.B., Widerlöv, E., Bissette, G., Walléus, H., Karlsson, I., Eklund, K., Kilts, C.D., Loosen, P.T., Vale, W., 1984. Elevated concentrations of CSF corticotropin-releasing factor-like immunoreactivity in depressed patients. *Science* 226 (4680), 1342–1344. <https://doi.org/10.1126/science.6334362>.
- Nestler, E.J., Carlezon Jr., W.A., 2006. The mesolimbic dopamine reward circuit in depression. *Biol. Psychiatry* 59 (12), 1151–1159. <https://doi.org/10.1016/j.biopsych.2005.09.018>.
- Nguyen, T., Wang, R., Russell, J.H., 2000. IL-12 enhances IL-2 function by inducing CD25 expression through a p38 mitogen-activated protein kinase pathway. *Eur. J. Immunol.* 30 (5), 1445–1452. [https://doi.org/10.1002/\(sici\)1521-4141\(200005\)30:5<1445::aid-immu1445>3.0.co;2-m](https://doi.org/10.1002/(sici)1521-4141(200005)30:5<1445::aid-immu1445>3.0.co;2-m).
- Palumbo, M.L., Canzobre, M.C., Pascuan, C.G., Ríos, H., Wald, M., Genaro, A.M., 2010. Stress induced cognitive deficit is differentially modulated in BALB/c and C57BL/6 mice: correlation with Th1/Th2 balance after stress exposure. *J. Neuroimmunol.* 218 (1–2), 12–20. <https://doi.org/10.1016/j.jneuroim.2009.11.005>.
- Palumbo, M.L., Trinchero, M.F., Zorrilla-Zubilete, M.A., Schinder, A.F., Genaro, A.M., 2012. Glatiramer acetate reverts stress-induced alterations on adult neurogenesis and behavior. Involvement of Th1/Th2 balance. *Brain Behav. Immun.* 26 (3), 429–438. <https://doi.org/10.1016/j.bbi.2011.12.006>.
- Pasciuto, E., Burton, O.T., Roca, C.P., Lagou, V., Rajan, W.D., Theys, T., Mancuso, R., Tito, R.Y., Kouser, L., Callaerts-Vegh, Z., et al., 2020a. Microglia require CD4 T cells to complete the fetal-to-adult transition. *Cell* 182 (3), e624. <https://doi.org/10.1016/j.cell.2020.06.026>, 625–640.
- Pasciuto, E., Burton, O.T., Roca, C.P., Lagou, V., Rajan, W.D., Theys, T., Mancuso, R., Tito, R.Y., Kouser, L., Callaerts-Vegh, Z., et al., 2020b. Microglia require CD4 T cells to complete the fetal-to-adult transition. *Cell* 182 (3), e624. <https://doi.org/10.1016/j.cell.2020.06.026>, 625–640.
- Peng, Z., Zhang, C., 2020. EPA is more effective than DHA to improve depression-like behavior, glia cell dysfunction and hippocampal apoptosis signaling in a chronic stress-induced rat model of depression, 21 (5). <https://doi.org/10.3390/ijms21051769>.
- Peng, Z., Zhang, C., Yan, L., Zhang, Y., Yang, Z., Wang, J., Song, C., 2020. EPA is more effective than DHA to improve depression-like behavior, glia cell dysfunction and hippocampal apoptosis signaling in a chronic stress-induced rat model of depression. *Int. J. Mol. Sci.* 21 (5). <https://doi.org/10.3390/ijms21051769>.
- Plastira, I., Bernhart, E., Joshi, L., Koyani, C.N., Strohmaier, H., Reicher, H., Malle, E., Sattler, W., 2020. MAPK signaling determines lysophosphatidic acid (LPA)-induced inflammation in microglia. *J. Neuroinflammation* 17 (1), 127. <https://doi.org/10.1186/s12974-020-01809-1>.
- Prajeeth, C.K., Dittrich-Breiholz, O., Talbot, S.R., Robert, P.A., Huehn, J., Stangel, M., 2018. IFN- $\gamma$  producing Th1 cells induce different transcriptional profiles in Microglia and astrocytes. *Front. Cell. Neurosci.* 12, 352. <https://doi.org/10.3389/fncel.2018.00352>.
- Prajeeth, C.K., Kronisch, J., Khoroshi, R., Knier, B., Toft-Hansen, H., Gudi, V., Floess, S., Huehn, J., Owens, T., Korn, T., et al., 2017. Effectors of Th1 and Th17 cells act on astrocytes and augment their neuroinflammatory properties, 14 (1), 204. <https://doi.org/10.1186/s12974-017-0978-3>.
- Rattazzi, Piras, Ono, Deacon, 2013. CD4<sup>+</sup> But not CD8<sup>+</sup> T cells revert the impaired emotional behavior of immunocompromised RAG-1-deficient mice. *Transl. Psychiatry*.
- Reiche, E.M., Morimoto, H.K., Nunes, S.M., 2005. Stress and depression-induced immune dysfunction: implications for the development and progression of cancer. *Int. Rev. Psychiatr.* 17 (6), 515–527. <https://doi.org/10.1080/02646830500382102>.
- Rincón, M., Enslin, H., Raingeaud, J., Reicht, M., Zaptou, T., Su, M.S., Xenit, L.A., Davis, R.J., Flavell, R.A., 1998. Interferon-gamma expression by Th1 effector T cells mediated by the p38 MAP kinase signaling pathway. *EMBO J.* 17 (10), 2817–2829. <https://doi.org/10.1093/emboj/17.10.2817>.
- Roque, A., Ochoa-Zarzosa, A., Torner, L., 2016. Maternal separation activates microglial cells and induces an inflammatory response in the hippocampus of male rat pups, independently of hypothalamic and peripheral cytokine levels. *Brain Behav. Immun.* 55, 39–48. <https://doi.org/10.1016/j.bbi.2015.09.017>.
- Séguin, R., Biernacki, K., Prat, A., Wosik, K., Kim, H.J., Blain, M., McCrea, E., Bar-Or, A., Antel, J.P., 2003. Differential effects of Th1 and Th2 lymphocyte supernatants on human microglia. *Glia* 42 (1), 36–45. <https://doi.org/10.1002/glia.10201>.
- Sánchez-Vidana, D.I., Po, K.K., Fung, T.K., Chow, J.K., Lau, W.K., So, P.K., Lau, B.W., Tsang, H.W., 2019. Lavender essential oil ameliorates depression-like behavior and increases neurogenesis and dendritic complexity in rats. *Neurosci. Lett.* 701, 180–192. <https://doi.org/10.1016/j.neulet.2019.02.042>.
- Sántha, P., Veszelka, S., Hoyk, Z., Mészáros, M., Walter, F.R., Tóth, A.E., Kiss, L., Kincses, A., Oláh, Z., Seprényi, G., et al., 2015. Restraint stress-induced morphological changes at the blood-brain barrier in adult rats. *Front. Mol. Neurosci.* 8, 88. <https://doi.org/10.3389/fnmol.2015.00088>.
- Salim, S., Chugh, G., Asghar, M., 2012. Inflammation in anxiety. *Adv. Protein Chem. Struct. Biol.* 88, 1–25. <https://doi.org/10.1016/b978-0-12-398314-5.00001-5>.
- Scheinert, R.B., Haeri, M.H., Lehmann, M.L., Herkenham, M., 2016. Therapeutic effects of stress-programmed lymphocytes transferred to chronically stressed mice. *Prog. Neuropsychopharmacol. Biol. Psychiatry* 70, 1–7. <https://doi.org/10.1016/j.pnpbp.2016.04.010>.
- Sha, Z., Xu, J., 2023. Regulatory Molecules of Synaptic Plasticity in Anxiety Disorder, vol. 16, pp. 2877–2886. <https://doi.org/10.2147/ijgm.s413176>.
- Shih, J.C., Chen, K., Ridd, M.J., 1999. Role of MAO A and B in neurotransmitter metabolism and behavior. *Pol. J. Pharmacol.* 51 (1), 25–29.
- Strachan-Whaley, M., Rivest, S., Yong, V.W., 2014. Interactions between microglia and T cells in multiple sclerosis pathobiology. *J. Interferon Cytokine Res.* 34 (8), 615–622. <https://doi.org/10.1089/jir.2014.0019>.
- Sun, L., He, C., Nair, L., Yeung, J., Egwuagu, C.E., 2015. Interleukin 12 (IL-12) family cytokines: role in immune pathogenesis and treatment of CNS autoimmune disease. *Cytokine* 75 (2), 249–255. <https://doi.org/10.1016/j.cyto.2015.01.030>.
- Wada, Y., Lu, R., Zhou, D., Chu, J., Przewlocka, T., Zhang, S., Li, L., Wu, Y., Qin, J., Balasubramanyam, V., et al., 2007. Selective abrogation of Th1 response by STA-5326, a potent IL-12/IL-23 inhibitor. *Blood* 109 (3), 1156–1164. <https://doi.org/10.1182/blood-2006-04-019398>.
- Wang, C., Li, Y., Yi, Y., Liu, G., Guo, R., Wang, L., Lan, T., Wang, W., Chen, X., Chen, S., et al., 2022. Hippocampal microRNA-26a-3p deficit contributes to neuroinflammation and behavioral disorders via p38 MAPK signaling pathway in rats. *J. Neuroinflammation* 19 (1), 283. <https://doi.org/10.1186/s12974-022-02645-1>.
- Wang, J., Wei, Q., Wang, C.Y., Hill, W.D., Hess, D.C., Dong, Z., 2004. Minocycline up-regulates Bcl-2 and protects against cell death in mitochondria. *J. Biol. Chem.* 279 (19), 19948–19954. <https://doi.org/10.1074/jbc.M313629200>.
- Wang, Y., Jia, Y., Zhao, W., Shao, Y., Zhang, Y., Chen, H., Qian, S., Hu, F., 2025. Hemerocallis citrina Baroni leaf total phenol alleviates depressive-like behaviors via modulating "microbiota-gut-brain" axis in chronic unpredictable mild stress-induced rats. *Front. Pharmacol.* 16, 1642515. <https://doi.org/10.3389/fphar.2025.1642515>.
- Weber, M.D., Godbout, J.P., Sheridan, J.F., 2017. Repeated social defeat, neuroinflammation, and behavior: monocytes carry the signal. *Neuropsychopharmacology* 42 (1), 46–61. <https://doi.org/10.1038/npp.2016.102>.
- Willner, P., 2017. The chronic mild stress (CMS) model of depression: history, evaluation and usage. *Neurobiol. Stress* 6, 78–93. <https://doi.org/10.1016/j.yfnstr.2016.08.002>.
- Wittenberg, G.M., Stylianou, A., Zhang, Y., Sun, Y., Gupta, A., Jagannatha, P.S., Wang, D., Hsu, B., Curran, M.E., Khan, S., et al., 2020. Effects of immunomodulatory drugs on depressive symptoms: a mega-analysis of randomized, placebo-controlled clinical trials in inflammatory disorders. *Mol. Psychiatr.* 25 (6), 1275–1285. <https://doi.org/10.1038/s41380-019-0471-8>.
- Wolf, S.A., Steiner, B., Akpınarlı, A., Kammertoens, T., Nassenstein, C., Braun, A., Blankenstein, T., Kempermann, G., 2009. CD4-positive T lymphocytes provide a neuroimmunological link in the control of adult hippocampal neurogenesis. *J. Immunol.* 182 (7), 3979–3984. <https://doi.org/10.4049/jimmunol.0801218>.
- Xiong, T., Zhang, Z., Zheng, R., Huang, J., Guo, L., 2019. N-acetyl cysteine inhibits lipopolysaccharide-induced apoptosis of human umbilical vein endothelial cells via the p38MAPK signaling pathway. *Mol. Med. Rep.* 20 (3), 2945–2953. <https://doi.org/10.3892/mmr.2019.10526>.
- Xu, J., Wang, B., Ao, H., 2025. Corticosterone effects induced by stress and immunity and inflammation: mechanisms of communication. *Front. Endocrinol.* 16, 1448750. <https://doi.org/10.3389/fendo.2025.1448750>.
- Ye, Q., Zeng, C., Luo, C., Wu, Y., 2020. Ferostatin-1 mitigates cognitive impairment of epileptic rats by inhibiting P38 MAPK activation. *Epilepsy Behav.* 103 (Pt A), 106670. <https://doi.org/10.1016/j.yebeh.2019.106670>.
- Yoshida, T.M., Nguyen, M., 2025. The Subfornical Organ is a Nucleus for gut-derived T Cells that Regulate Behaviour. <https://doi.org/10.1038/s41586-025-0905-7>.
- Zarif, H., Hosseiny, S., Paquet, A., Lebrignand, K., Arguel, M.J., Cazarreth, J., Lazzari, A., Heurteaux, C., Glaichenhaus, N., Chabry, J., et al., 2018. CD4(+) T cells have a permissive effect on enriched environment-induced hippocampal synaptic plasticity. *Front. Synaptic Neurosci.* 10, 14. <https://doi.org/10.3389/fnsyn.2018.00014>.
- Zhang, C., Zhang, Y., Li, Y., Liu, B., Wang, H., Li, K., Zhao, S., Song, C., 2019a. Minocycline ameliorates depressive behaviors and neuro-immune dysfunction induced by chronic unpredictable mild stress in the rat. *Behav. Brain Res.* 356, 348–357. <https://doi.org/10.1016/j.bbr.2018.07.001>.
- Zhang, C., Zhang, Y.P., Li, Y.Y., Liu, B.P., Wang, H.Y., Li, K.W., Zhao, S., Song, C., 2019b. Minocycline ameliorates depressive behaviors and neuro-immune dysfunction induced by chronic unpredictable mild stress in the rat. *Behav. Brain Res.* 356, 348–357. <https://doi.org/10.1016/j.bbr.2018.07.001>.
- Zhang, J., He, H., Qiao, Y., Zhou, T., He, H., Yi, S., Zhang, L., Mo, L., Li, Y., Jiang, W., et al., 2020. Priming of microglia with IFN- $\gamma$  impairs adult hippocampal neurogenesis and leads to depression-like behaviors and cognitive defects, 68 (12), 2674–2692. <https://doi.org/10.1002/glia.23878>.
- Zhang, S., Kaplan, M.H., 2000. The p38 mitogen-activated protein kinase is required for IL-12-induced IFN-gamma expression. *J. Immunol.* 165 (3), 1374–1380. <https://doi.org/10.4049/jimmunol.165.3.1374>.
- Zhao, H., Wan, L., Chen, Y., Zhang, H., Xu, Y., Qiu, S., 2018. FasL incapacitation alleviates CD4(+) T cells-induced brain injury through remodeling of microglia polarization in mouse ischemic stroke. *J. Neuroimmunol.* 318, 36–44. <https://doi.org/10.1016/j.jneuroim.2018.01.017>.
- Zhao, J., Liu, J., Denney, J., Li, C., Li, F., Chang, F., Chen, M., Yin, D., 2015. TLR2 involved in naive CD4<sup>+</sup> T cells rescues stress-induced immune suppression by regulating Th1/Th2 and Th17. *Neuroimmunomodulation* 22 (5), 328–336. <https://doi.org/10.1159/000371468>.
- Zhu, C.B., Lindler, K.M., Owens, A.W., Daws, L.C., Blakely, R.D., Hewlett, W.A., 2010. Interleukin-1 receptor activation by systemic lipopolysaccharide induces behavioral despair linked to MAPK regulation of CNS serotonin transporters. *Neuropsychopharmacology* 35 (13), 2510–2520. <https://doi.org/10.1038/npp.2010.116>.
- Ziv, Y., Ron, N., Butovsky, O., Landa, G., Sudai, E., Greenberg, N., Cohen, H., Kipnis, J., Schwartz, M., 2006. Immune cells contribute to the maintenance of neurogenesis and spatial learning abilities in adulthood. *Nat. Neurosci.* 9 (2), 268–275. <https://doi.org/10.1038/nn1629>.